Structure-Based Generation of a New Class of Potent Cdk4 Inhibitors: New *de Novo* Design Strategy and Library Design

Teruki Honma,* Kyoko Hayashi, Tetsuya Aoyama, Noriaki Hashimoto, Takumitsu Machida, Kazuhiro Fukasawa, Toshiharu Iwama, Chinatsu Ikeura, Mari Ikuta, Ikuko Suzuki-Takahashi, Yoshikazu Iwasawa, Takashi Hayama, Susumu Nishimura, and Hajime Morishima

Banyu Tsukuba Research Institute in collaboration with Merck Research Laboratories, Okubo-3, Tsukuba 300-2611, Ibaraki, Japan

As a first step in structure-based design of highly selective and potent Cdk4 inhibitors, we performed structure-based generation of a novel series of Cdk4 inhibitors. A Cdk4 homology model was constructed according to X-ray analysis of an activated form of Cdk2. Using this model, we applied a new *de novo* design strategy which combined the *de novo* design program LEGEND with our in-house structure selection supporting system SEEDS to generate new scaffold candidates. In this way, four classes of scaffold candidates including diarylurea were identified. By constructing diarylurea informer libraries based on the structural requirements of Cdk inhibitors in the ATP binding pocket of the Cdk4 model, we were able to identify a potent Cdk4 inhibitor *N*-(9-oxo-9*H*-fluoren-4-yl)-*N*-pyridin-2-ylurea **15** (IC$_{50}$ = 0.10 μM), together with preliminary SAR. We performed a docking study between **15** and the Cdk4 model and selected a reasonable binding mode which is consistent with the SAR. Further modification based on the proposed binding mode provided a more potent compound, *N*-[(9b*R*)-5-oxo-2,3,5,9b-tetrahydro-1*H*-pyrrolo[2,1-*a*]isoindol-9-yl]-*N*-pyridin-2-ylurea **26a** (IC$_{50}$ = 0.042 μM), X-ray analysis of which was accomplished by the soaking method. The predicted binding mode of **15** in Cdk4 was validated by X-ray analysis of the Cdk2−**26a** complex.

Introduction

Cyclins and cyclin-dependent kinases (Cdks) play important roles in regulation of the cell cycle.[1] In particular, D-type cyclins, which are activated by rearrangement or amplification in several tumors,[2] associate with Cdk4/6. Cyclin D−Cdk4/6 complexes phosphorylate the retinoblastoma protein (pRB) and regulate the cell cycle during G$_1$/S transition.[3] Loss of function or deletion of p16^{ink4a} (an endogenous Cdk4/6 specific inhibitor protein) frequently occurs in clinical cancer cells.[4]

Several Cdk inhibitors such as UCN-01,[5] flavopiridol,[6] purvalanol B,[7] pyrido[2,3-*d*]pyrimidin-7-one,[8] and indenopyrazole[9] have been reported. Among these, nonspecific Cdk inhibitors, UCN-01 and flavopiridol, have entered clinical trials. As a next generation of Cdk inhibitors, selective inhibitors of only one target Cdk are expected to cause cell cycle arrest specifically.[10] Suppression of tumor growth by G$_1$ arrest is thought to reduce the stress for normal cells more than in other phases, because normal cells are usually resting in the G$_0$-G$_1$ phase. Therefore, we tried to design Cdk4 selective inhibitors that cause cell cycle arrest in the G$_1$ phase.

To obtain highly selective and potent Cdk4 inhibitors, we performed a structure-based design consisting of the following two steps: (1) lead generation of a new class of Cdk4 inhibitors based on a Cdk4 homology model and (2) enhancement of Cdk4 selectivity of lead compounds over Cdk1/2 and the other kinases based on the binding modes and structural differences between Cdk4 and other kinases. In this paper, we describe structure-based lead generation as a first step. The results of lead optimization to improve Cdk4 selectivity will be reported in an accompanying article.

Recently, several successful examples of structure-based lead generation such as the HIV-1 integrase inhibitor, FKBP-12 ligand, Factor Xa inhibitor, COX-2 inhibitor, and DNA gyrase inhibitor have been reported.[11] In most cases, methods for structure-based lead generation were based on computational descriptions of a binding site, as in the coordinates of atoms or pharmacophores, and also based on techniques to search for the configurational and conformational space of a candidate molecule in the binding site, evaluating potential energy and/or scoring of binding affinity. These methods are classified into two categories: 3D database search[12] and *de novo* design.[13] In the case of 3D database search, programs such as DOCK,[14] UNITY,[15] and Catalyst[16] take each molecule from known compound databases and attempt to position it in the active site of a receptor or pharmacophore model. Three-dimensional database search is more frequently used because hit compounds are just listed in the commercial catalogues or synthetically accessible. However, most 3D database search programs have one or more of the following critical problems: (1) the number of considered conformations for each ligand is often not sufficient, (2) some functional groups work as the ionic form in a physiological condition (pH 7.4), whereas 3D database search programs often use their neutral forms, and (3) novel structures cannot be obtained. On the other hand, *de novo* design programs such as LEGEND,[17] LeapFrog,[18] CONCERTS,[19] PRO-LIGAND,[20] and LUDI[21] sequentially build up structures which are predicted to fit the

* To whom correspondence should be addressed. Tel: 81-298-77-2000. Fax: 81-298-77-2029. E-mail: honmatr@banyu.co.jp.

Table 1. Reported X-ray Analyses of the Cdk Family and Hydrogen-Bonding Sites Used by Small Ligands[23–25,29–33]

PDB ID	molecule	hydrogen-bonding sites used by small ligands								
		E81 CO	L83 NH	L83 CO	K33 NζH	D86 Oδ	Q131 Oε	D145 Oδ	N132 Oδ	Wat74[a]
1HCL	Cdk2									
1B39	Cdk2[c]-ATP	NH	N		PO		OH			
1HCK	Cdk2-ATP	NH	N		PO	OH	OH			
1FIN	Cdk2-ATP-cyclin A₂	NH	N							
1JST	Cdk2[c]-ATP[b]-cyclin A₂	NH	N		PO					PO
1QMZ	Cdk2[c]-ATP[f]-cyclin A₂-substrate[d]	NH	N		PO	OH	OH			
1DM2	Cdk2-hymenialdisine	NH	CO	NH					NH	CO
1CKP	Cdk2-Purvalanol B		N	NH						
	Cdk2-L828276[e]	OH	CO		OH			NH⁺,OH		OH
	Cdk2-isopentenyladenyne	NH	N		N					
	Cdk2-olomoucine		N	NH			OH			
	Cdk2-roscovitine		N	NH						
1AQ1	Cdk2-staurosporin	NH	CO			NH⁺				
1BUH	Cdk2-Ckshs1									
1JSU	Cdk2-cyclinA₂-p27									
1BI7	Cdk6-p16									
1BI8	Cdk6-p19									
1BLX	Cdk6-p19									

[a] Wat74 is a water molecule in 1JST. [b] ATPγS. [c] Thr160 phosphorylated Cdk2. [d] Substrate peptide (HHASPRK). [e] *des*-Chloroflavopiridol. [f] AMPPNP.

active site of the receptor. In the case of *de novo* design, considering conformations and forms of functional groups would not be critical problems, because *de novo* design programs generate functional groups in suitable forms and suitable conformations to interact with the protein surface. Furthermore, *de novo* design programs can also construct structures including novel skeletons. We applied this *de novo* design strategy to discover novel lead compounds. However, in contrast to structures obtained from 3D database search programs, output structures obtained from *de novo* design programs usually have greater difficulty in commercial availability and synthetic feasibility.

To overcome these problems in the conventional *de novo* design strategies, we constructed the chemical structure selection supporting system, SEEDS (system for evaluation of availability of essential structures generated by *de novo* ligand design programs),[22] taking advantage of database searches. The program SEEDS automatically extracts an essential part of each structure by the *de novo* design program, and searches for commercially available and/or synthetically accessible derivatives of the essential parts. In this study, we used the *de novo* design program LEGEND with this SEEDS to generate novel scaffold candidates with molecular weights of less than 350.

After the discovery of some promising scaffold candidates, it is important to validate whether the scaffold candidates bind to Cdk4 in desired ways. Recently, efficient validation methods based on NMR analysis have been reported (SAR by NMR[11c] and needle screening[11f]). However, the molecular weight of Cdk4 (44 kDa) is so large that measurement of its NMR is not feasible. Thus, we synthesized several informer libraries of a scaffold and, using the preliminary structure–activity relationship (SAR), validated the binding mode by molecular modeling methods. Then modifications based on the predicted binding mode were performed to discover more potent lead compounds.

Results and Discussion

Homology Modeling of Cdk4 Based on the X-ray Structure of Cdk2. X-ray analyses of the Cdk family are summarized in Table 1. In 1993, the first X-ray analysis of monomeric Cdk2 was reported by H. L. De Bondt et al.[23] In 1996, the structure of the Thr160 phosphorylated Cdk2-cyclin A-ATPγS complex, a final activated form of Cdk2, was solved by A. A. Russo et al.[24] They revealed the activation mechanism of Cdk2 by analyzing conformational changes with cyclin A and phosphorylation of Thr160. Although the structures of the Cdk6–p16 complex and Cdk6–p19 complex were already known, their cyclin binding region and the ATP binding pocket in Cdk6 were both largely altered by the endogenous inhibitors, p16 or p19.[25] Therefore, despite a very high sequence identity between Cdk4 and Cdk6 (70%), we could not use these structural data for designing Cdk4 inhibitors. On the other hand, the level of sequence homology between Cdk4 and Cdk2 is quite high (45%) so that it seemed appropriate to construct a Cdk4 model based on the final activated form of Cdk2 (Protein Data Bank (PDB) ID: 1JST).

According to the sequence alignments by S. K. Hanks et al.,[26] we constructed an initial Cdk4 model using the modeling software BIOCES[E].[27] The model was minimized with the CHARMm (Chemistry at Harvard Molecular mechanics) force field[28] with the exception of the conserved region in Cdk4 and Cdk2. This minimized structure was used for scaffold design in the *de novo* design strategy.

Structure-Based Generation of New Scaffold Candidates. According to several binding modes of ATPγS and ATP competitive Cdk2 inhibitors determined by X-ray analysis, we examined the structural requirements for binding of the inhibitors in the ATP binding pocket (Table 1). In Cdk2, the main chain NH group in Leu83 would be the most important in binding of the inhibitors because it serves as a hydrogen-bonding donor in every structure reported so far. The main chain carbonyl groups of Glu81 and Leu83 also seemed to be important because most inhibitors form a hydrogen bond(s) with them. In addition, Lys33 NζH, Asp86 Oδ, Glu131 Oε, and a highly conserved water molecule (Wat74 in 1JST) are utilized by some ligands. In terms of hydrophobicity, some areas deep in the ATP binding pocket around Glu81 and Leu83 are occupied by flat aromatic rings of Cdk2 inhibitors, such as flavopiridol,[29] staurosporin,[30] and roscovitine.[31] Indeed, these areas
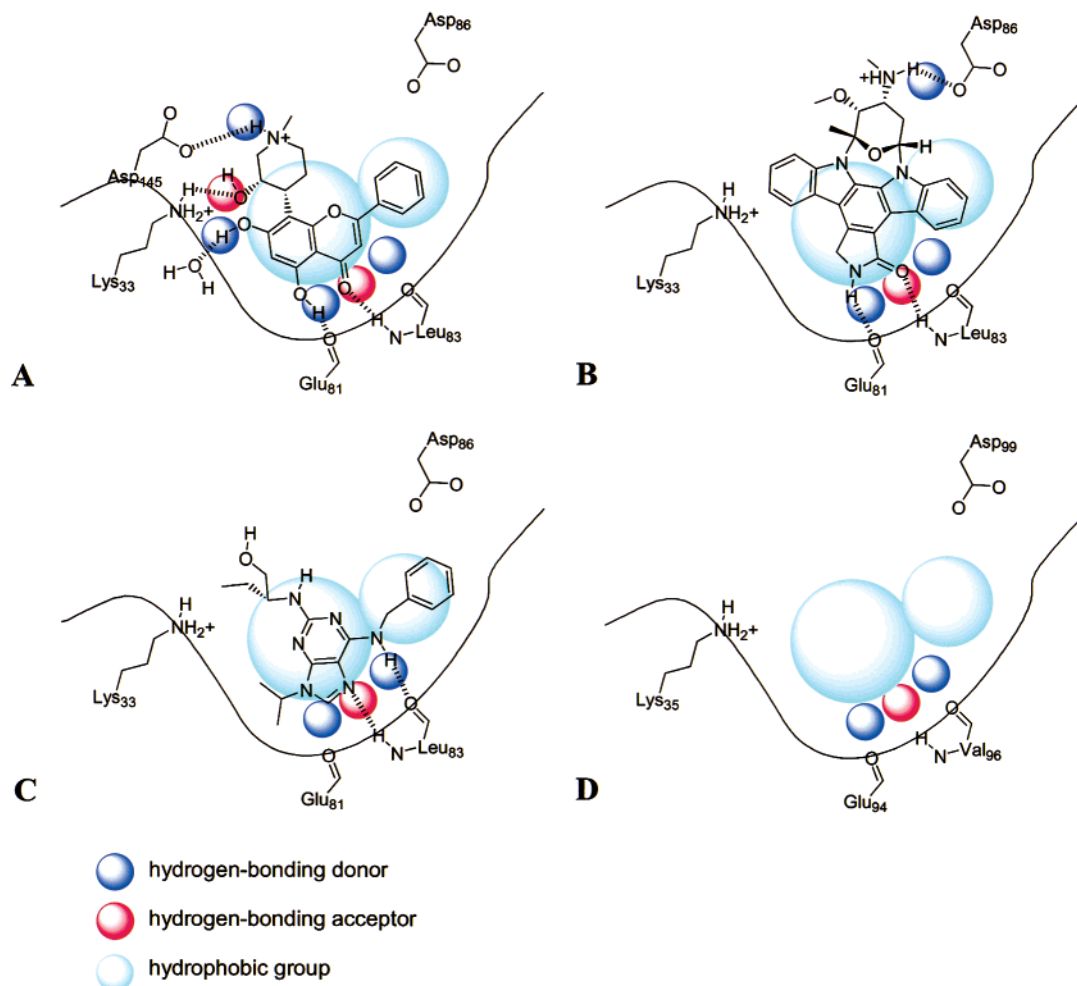
Figure 1. Structural requirements of ATP-competitive Cdk inhibitors. A: L828276 (*des*-chloroflavopiridol)−Cdk2 complex.[29] B: staurosporin−Cdk2 complex (1AQ1 in PDB).[30] C: roscovitine−Cdk2 complex.[31] D: predicted structural requirements in the Cdk4 homology model.

are surrounded by the hydrophobic amino acid residues Ile10, Val18, Ala31, Val64, Phe80, Phe82, Leu134, and Ala144 and form a narrow cavity. The binding modes of representative Cdk2 inhibitors and the locations of the pharmacophores are shown schematically in Figure 1A−C. In Cdk4, most of the residues that are important for hydrogen bonds or hydrophobic interactions are conserved according to Hanks' multiple alignment. Among the altered amino acid residues, those between Leu83 in Cdk2 and Val96 in Cdk4 would not be critical since only the main chain is used for hydrogen bond(s). Therefore, we considered that the information concerning these structural requirements is also useful for discovering a new class of Cdk4 inhibitors.

To identify new scaffolds that satisfy these structural requirements, we applied a *de novo* design program, LEGEND. This program is based on the atom-by-atom approach[34] and is suitable for generation of drug molecules in a deep, narrow cavity just like the ATP binding pocket. With this program, we can specify the directions of growth, the size of the molecules that will be generated, and the hydrogen bonds that will be formed during calculations. Specification of the calculation performed by LEGEND and the process of scaffold generation are shown in Scheme 1.

At a primary step, we obtained 1000 output structures; however, most of them were neither commercially available nor synthetically feasible. This problem appears to apply to most *de novo* design programs that build up structures sequentially. To overcome this disadvantage, we developed an in-house program, SEEDS.[22] The program SEEDS automatically picks out an essential substructure of each output from LEGEND and uses it in search of commercially available and/or synthetically feasible derivatives. This process is outlined in Figure 2 using an example. Structure **I** is one of the output structures generated by LEGEND. If we searched compound databases using structure **I** itself as a query, no commercially available derivatives could be obtained because of simple alkyl side chains which would not form hydrogen bonds. Therefore, SEEDS extracted rings and functional groups that were predicted to form hydrogen bonds as an essential structure (**II**). Subsequently, based on structure **II**, several queries for searching compound databases and reaction databases were automatically made by SEEDS. Query **III** is one of the examples for searching compound databases. Using the queries made by SEEDS, we first searched for commercially available derivatives. When attractive scaffold candidates from commercially available derivatives were not identified, we searched for synthetically feasible derivatives using reaction databases. On searching the Available Chemicals Directory (ACD),[35] 4884 compounds with molecular weights of less
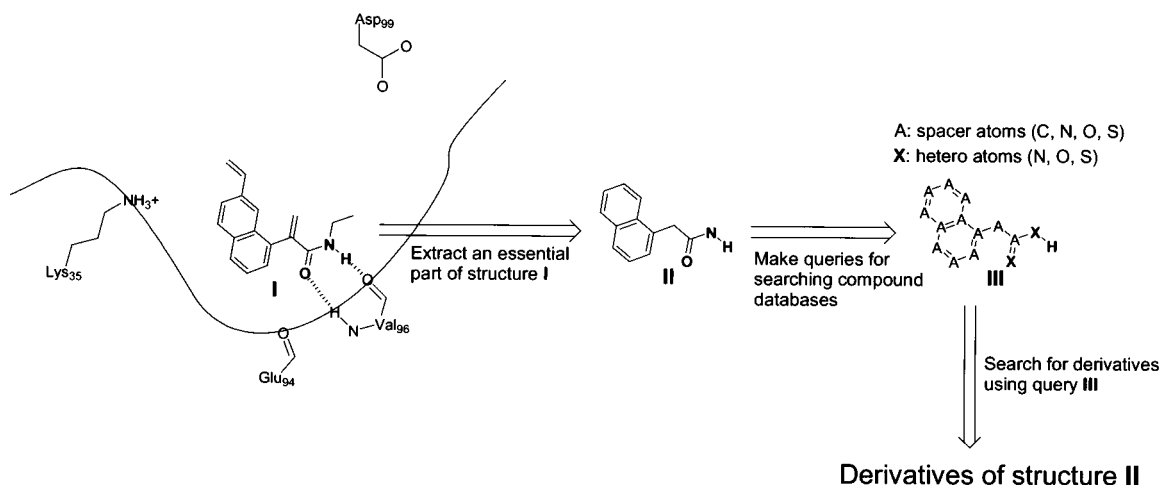
Figure 2. Schematic figure of the SEEDS. **I**: one of the output structures generated by the LEGEND. **II**: an essential part of structure **I**. **III**: one of the queries for searching compound databases.

**Scheme 1.** Process of Structure-Based Scaffold Generation
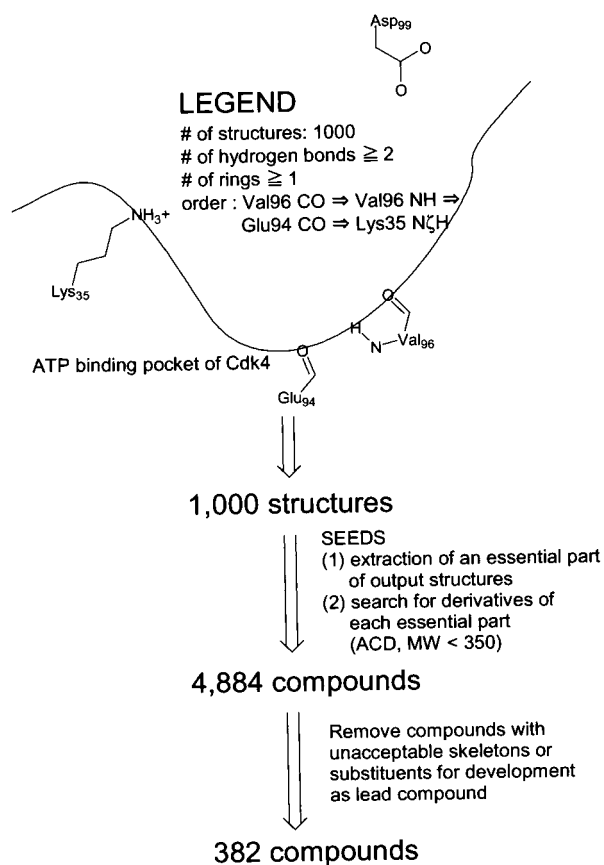
than 350 were selected. Compounds with skeletons or functional groups that were unacceptable for the development of lead compounds were omitted, and finally 382 commercially available compounds remained. The compounds were purchased for screening in cyclin D–Cdk4 assays at concentrations up to 1 mM. We obtained 18 compounds with IC_{50} values of under 500 μM as hits. Most of the hits had large, flat aromatic rings and a couple of neighboring hydrogen-bonding donors and acceptors. Twelve of the 18 hits were clustered into one of the following four classes according to their structural profile: diarylurea, cyclic urea and thiourea, 4-aryl-2-aminopyridine and triazine, and pteridine (Figure 3).
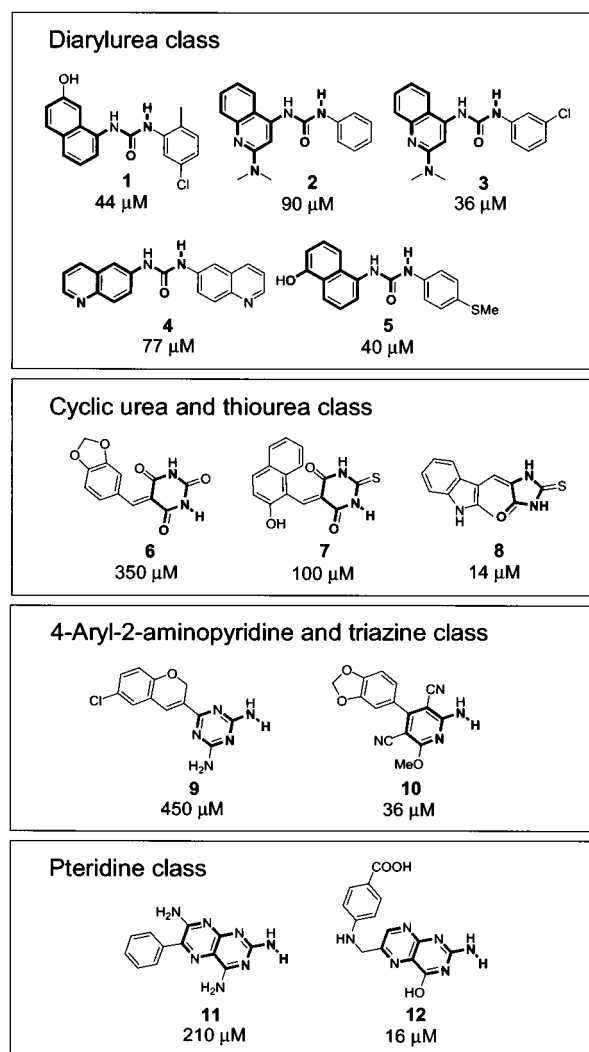
Figure 3. Typical classes of hit compounds and their IC_{50} values in cyclin D–Cdk4 assay. Bold lines represent essential parts of output structures by LEGEND.

In these four classes, our interest was directed to the diarylurea scaffold, because there were five potent compounds, **1**, **2**, **3**, **4**, and **5**, with a diarylurea structure that is appropriate for rapid construction of structurally diverse libraries. Therefore, we constructed diarylurea
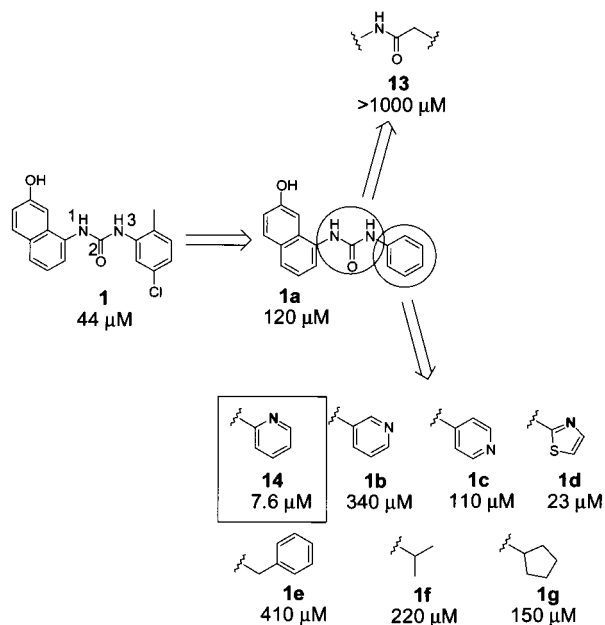
Figure 4. Diarylurea informer library (**1**): transformation of 5-chloro-2-methylphenyl group.

Table 2. Diarylurea Informer Library (2): Transformation of 7-Hydroxynaphthyl Group

no.	R	IC$_{50}$ (μM)	no.	R	IC$_{50}$ (μM)
15		0.10	14		7.6
14a		0.67	14d		100
14b		2.4	14e		>100
14c		3.6	14f		>100

informer libraries by parallel synthesis to validate the potential of the scaffold and to obtain preliminary SAR.

Construction of Diarylurea Informer Libraries. The data obtained through LEGEND suggested that neighboring NH and CO in the diarylurea scaffolds form hydrogen bond(s) with the main chain(s) of Glu94 and/or Val96, and aromatic rings are supposed to be located in the hydrophobic regions as shown in Figure 1. According to these insights, we designed informer libraries as described below.

First, we searched for substituents for the 5-chloro-2-methylphenyl group in the diarylurea **1**, leaving the 7-hydroxynaphthyl group intact. Considering the deep, narrow shape of the ATP binding pocket, we mainly selected flat aromatic amines as building blocks to synthesize diarylurea derivatives. Fifty-five urea compounds were synthesized from 8-isocyanato-2-naphthol and alkylamines in moderate yields (30−70%). In addition, we prepared an amide compound **13** to confirm the importance of the urea moiety. The resultant SAR is summarized in Figure 4. Substitutions with 2-pyridinyl (**14**) and 2-thiazolyl (**1d**) groups gave IC$_{50}$ values of 7.6 μM and 23 μM, respectively, while substitutions with 3-pyridinyl (**1b**) and 4-pyridinyl (**1c**) groups showed poor inhibitory activities. The relative position of the nitrogen atom in the aromatic ring seemed to be important for binding of the inhibitor. None of the compounds substituted with aliphatic amines showed enhanced potency. Transformation of NH-3 (numbering of atoms is shown in Figure 4) into CH$_2$ (**13**) caused a remarkable decrease in Cdk4 inhibition. These SAR suggested (1) the nitrogen atom on 2-substituted pyridine and 2-substituted thiazole form a hydrogen bond with protein or an intramolecular hydrogen-bonding site (i.e., NH-1 of the urea moiety) and (2) the NH-3 of the urea moiety is important as a hydrogen-bonding donor.

Next we kept the 2-pyridinyl group intact and modified the 7-hydroxynaphthyl group in compound **14**. The 7-hydroxynaphthyl group was predicted to be located in the hydrophobic, narrow, deep area of the ATP

binding pocket. Therefore, as in the case of the first informer library, we mainly selected aromatic amines as building blocks. Using these building blocks, 410 urea compounds were synthesized and tested by Cdk4 inhibitory assay. These compounds were provided by the coupling reaction between alkylamines and pyridine-2-carbonyl azide. The structures and assay results for representative compounds are summarized in Table 2. This area required an aromatic ring, because none of the aliphatic substituted compounds showed inhibitory activity (**14e** and **14f** are representatives). The existence of a hydrogen-bonding acceptor in the left part (**14a**−**c** and **15**) led to a significant improvement of potency, in particular, with compound **15** (IC$_{50}$ = 0.10 μM). Compound **15** was selected as the lead compound for further modification.

Prediction of the Binding Mode of Diarylurea 15 in Cdk4. To investigate the binding mode of **15** more comprehensively, we performed a docking study between the Cdk4 model and **15**. First we made 400 conformations of the Cdk4−**15** complex model by manual docking, random sampling, and minimization with the modeling software QUANTA.[36] These conformations were clustered by root-mean-square deviation (RMSD) of atomic coordinates (40 clusters), and representative conformations in each cluster with the lowest energy in the CHARMm force field were extracted. Then, the representative conformations were filtered by the following two conditions based on structural requirements for being ATP competitive Cdk inhibitors as shown in Figure 1: (1) the NH group of Val96 forms a hydrogen bond with **15** and (2) the aromatic ring(s) of **15** is located in the hydrophobic regions. Four patterns of binding modes were suggested (Figure 5A−D).

In all candidates, formation of an intramolecular hydrogen bond between urea NH-1 (numbering of atoms is shown in Figure 6) and the nitrogen atom (N-5) on the pyridine ring was predicted (Table 3), and the fluorenone moiety was located in the hydrophobic region in Figure 1. According to SAR of the informer libraries,
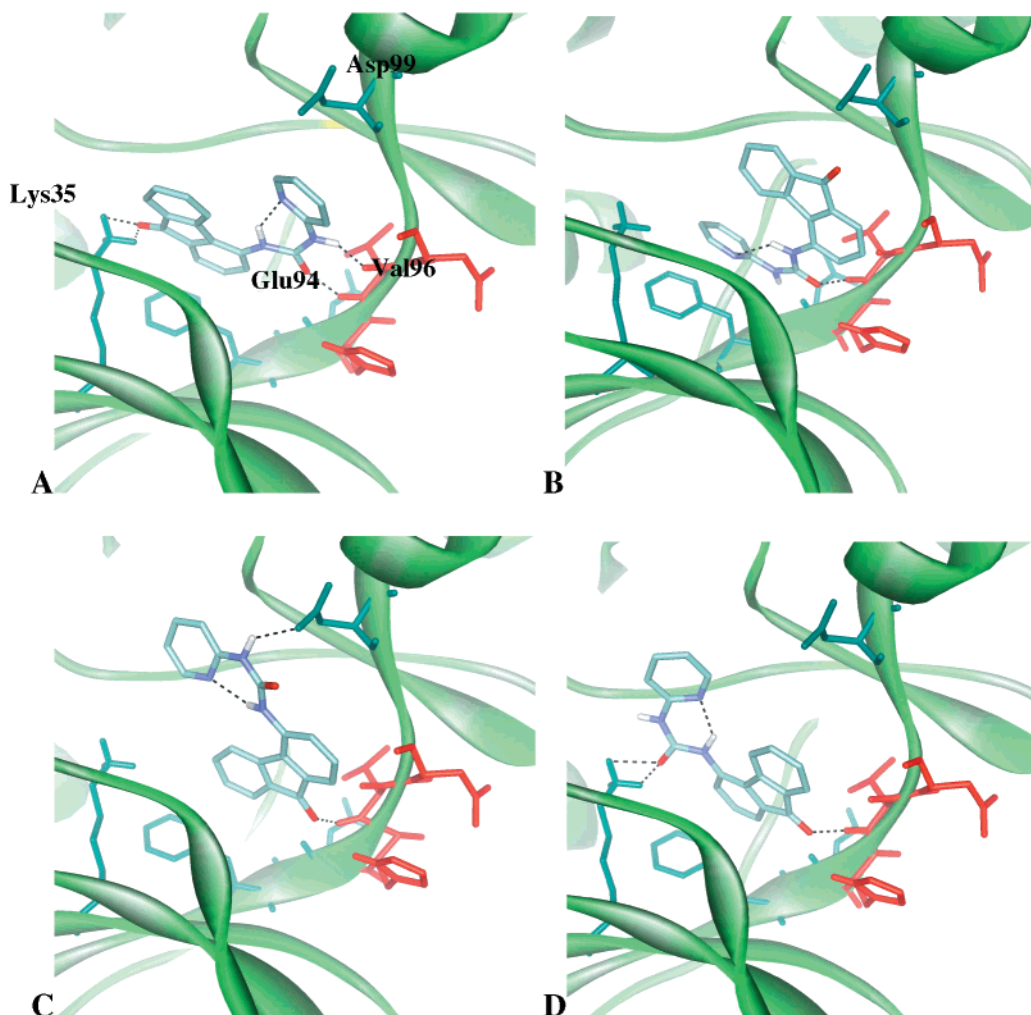
Figure 5. Four predicted binding mode candidates of **15** in the Cdk4 model. Right green ribbon: ribbon representation of the Cdk4 model. Green residues: conserved amino acid residues in Cdk4 and Cdk2. Red residues: different amino acid residues in Cdk4 and Cdk2. Broken lines: predicted hydrogen bonds.
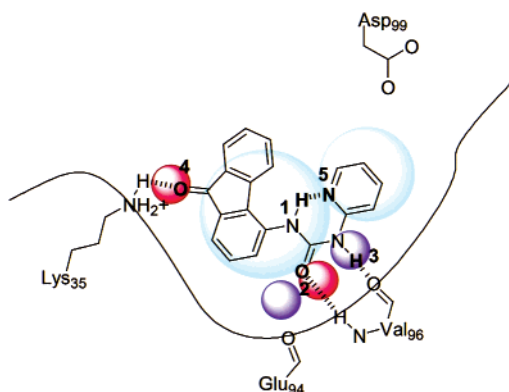
Figure 6. Schematic figure of mode A.

Table 3. Predicted Hydrogen Bonds in the Binding Mode Candidates[a]

binding mode candidates	hydrogen-bonding sites				
	CO-4	NH-1	CO-2	NH-3	N-5
mode A	Lys35 NζH	N-5	Val96 NH	Val96 CO	NH-1
mode B		N-5	Val96 NH		NH-1
mode C	Val96 NH	N-5		Asp99 Oδ	NH-1
mode D	Val96 NH	N-5	Lys35 NζH		NH-1

[a] Numbering of atoms at hydrogen-bonding sites is shown in Figure 5. Judgment of formation of hydrogen bonds was performed by QUANTA.

we were able to propose additional hypotheses for the validation of the binding modes as follows: (1) NH-3 of the urea moiety makes a hydrogen bond with the protein and (2) fluorenone CO-4 makes a hydrogen bond with the protein. Modes B and D could not satisfy these hypotheses at the same time, whereas modes A and C satisfied them simultaneously.

Next, we made a comparison of modes A and C. In mode A, the neighboring CO-2 and NH-3 formed two hydrogen bonds with the main chain of Val96, and both fluorenone and pyridine were located in accord with hydrophobic requirements (Figure 6). Compared to mode A, CO-2 in mode C could not make a hydrogen bond with any residues, and the pyridine ring deviated from the locations for hydrophobic requirements. Therefore, we concluded that mode A was preferable to mode C.

Design and Synthesis Based on the Predicted Binding Mode. In most conformations containing the cluster of mode A, the angle between the fluorenone and the pyridine was rather large (>30°) even in the narrow cavity. This suggests some degree of steric repulsion between the pyridine ring and the terminal benzene ring in the fluorenone. The large angle caused by the repulsion was supposed to be unfavorable for binding affinity. On the other hand, the terminal benzene ring
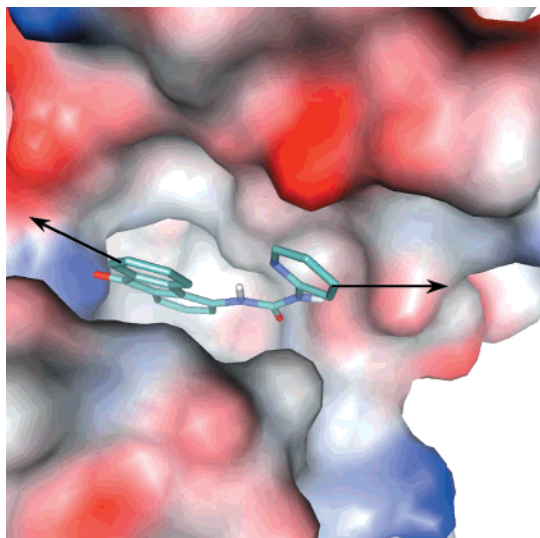
Figure 7. Suitable directions to introduce substituents in mode A. Cdk4 model: solvent accessible surface (probe: 1.4 Å) representation (colored by partial charge) by WebLab viewer. **15**: stick representation.
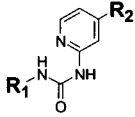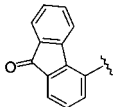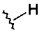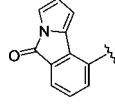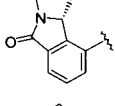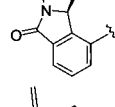
in the fluorenone was supposed to be important for binding affinity in mode A since the terminal benzene ring was appropriately located on the hydrophobic surface of Cdk4 (Figure 7).
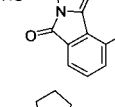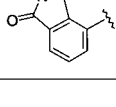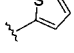
From these assumptions, we attempted to replace the terminal benzene ring with various kinds of five-membered rings in order to eliminate unnecessary intramolecular steric repulsion while maintaining favorable hydrophobic interactions. Representative compounds **25**, **26a**, and **26b** and their IC$_{50}$ values are shown in Table 4, and their synthetic routes are summarized in Scheme 2. Fused pyrrole **19** was synthesized by the intramolecular Heck reaction.[37] Reduction of **19** by Fe/HCl provided **23**. Saturated chiral amines **21a** and **21b** were obtained by hydrogenation with Pd/C and separation using chiral HPLC. The absolute configuration of **21b** was determined by X-ray analysis of the (−)-camphanic amide of **21b**. Compounds **25**, **26a**, and **26b** were synthesized by coupling reactions between these amines and pyridine-2-carbonyl azide. These modifications provided potent compounds with IC$_{50}$ values of up to 0.034 μM.

According to mode A, we also found some space for the introduction of substituents on the aromatic rings. We introduced substituents in the two positions shown by arrows in Figure 7. As a result, **27** with a substituent at the 5-position of the terminal pyrrole ring in **25** showed an IC$_{50}$ value of 0.017 μM, and **28** with 2-thiophene at the 4-position of the pyridine showed an IC$_{50}$ value of 0.011 μM. We performed docking studies between the Cdk4 model and **27/28** and recognized that the molecules were not able to bind to Cdk4 in the way of mode B, C, or D. This suggested that mode A would be the best candidate.

Confirmation of the Predicted Binding Mode by X-ray Analysis. For further validation of the binding mode, we tried X-ray analysis of the Cdk2−**15** complex by the soaking method. However, compound **15** was so insoluble (solubility at pH 7.4 in Tris-Cl buffer, <0.01 μg/mL) that soaking was not appropriate. During modification of **15**, we obtained a relatively soluble compound

**Table 4.** Designed Compounds and Their IC$_{50}$ Values in Cyclin D−Cdk4 Assay

no.	R$_1$	R$_2$	IC$_{50}$ (μM)
15		H	0.10
25		H	0.034
26a		H	0.042
26b		H	0.19
27		H	0.017
28			0.011

26a (solubility at pH 7.4 in Tris-Cl buffer, 7.18 μg/mL) with potent binding affinity. By using compound **26a**, we succeeded in X-ray analysis of the Cdk2−**26a** complex (PDB ID: 1GIH).[38] A comparison between mode A and the X-ray structure is shown in Figure 8. The X-ray analysis showed that **26a** formed hydrogen bonds with the main chain NH and CO groups of Leu83 (corresponding to Val96 in Cdk4) and adopted a U-shaped conformation in the ATP binding pocket of Cdk2. This binding mode of **26a** in Cdk2 (Figure 8B) was found to be consistent with the predicted binding mode of **15** in Cdk4 (mode A, Figure 8A).

Supported by the results of the docking study with the Cdk4 model, X-ray analysis of the Cdk2 complex, and the SAR obtained by the Cdk4 inhibitory assay, we concluded that mode A was the most preferable binding mode of the diarylurea series of lead compounds in the activated form of the cyclin D−Cdk4 complex.

Conclusion

We employed a structure-based lead generation approach consisting of the following steps: (1) homology modeling of the target protein, (2) scaffold generation by using the *de novo* design program LEGEND and our in-house structure selection supporting system SEEDS, (3) construction of informer libraries, and (4) structural modification based on the predicted binding mode. From the result, we developed a novel diarylurea class of potent inhibitor, **26a** (IC$_{50}$ = 0.042 μM). Combination

Scheme 2. Synthetic Routes of Diarylurea Derivatives **25**, **26a**, **26b**, **27**, and **28**[a]
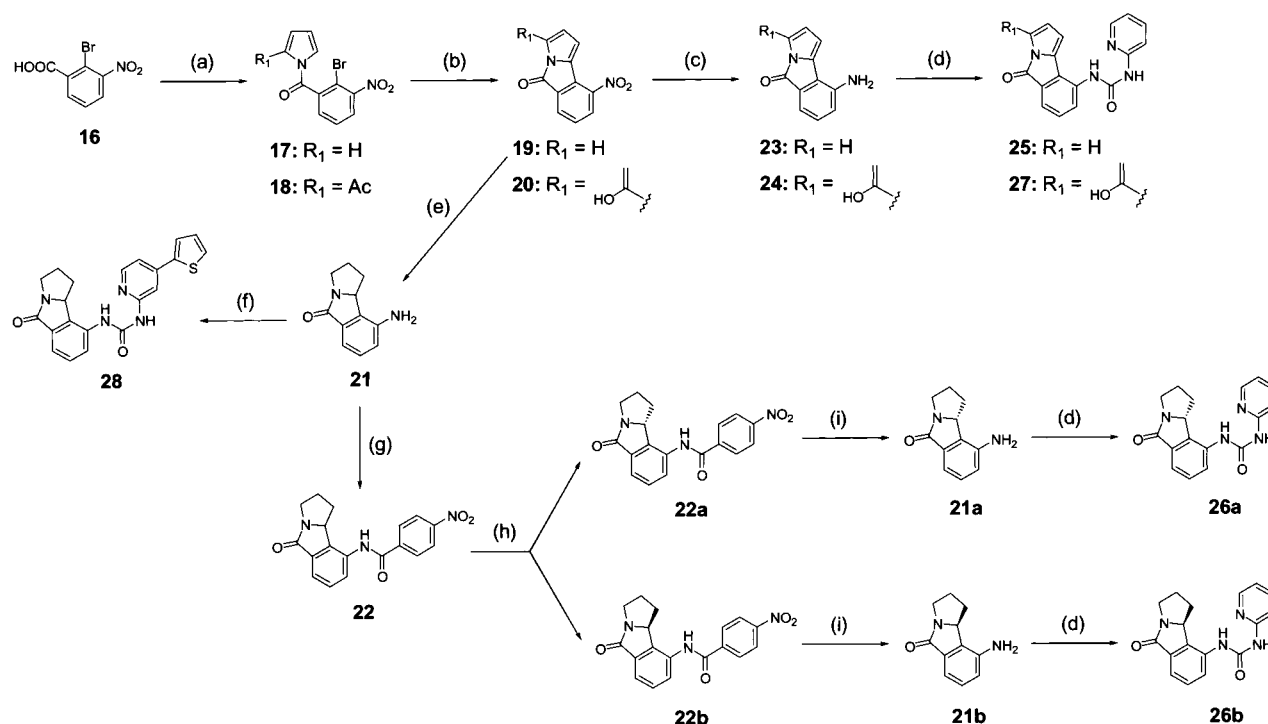
a Reagents: (a) (1) thionyl chloride; (2) pyrrole (for **17**) or 2-acetylpyrrole (for **18**), triethylamine, CH$_2$Cl$_2$, 36% (for **17**), 67% (for **18**); (b) Pd(PPh$_3$)$_4$, KOAc, dimethylacetamide, 81% (for **19**), 62% (for **20**); (c) Fe, 6 N HCl, MeOH, 83% (for **23**) or Pd/C, H$_2$, MeOH−tetrahydrofuran, 100% (for **24**); (d) pyridine-2-carbonyl azide, tetrahydrofuran, 30−70%; (e) Pd/C, H$_2$, MeOH, 99%; (f) (1) 4-tributylstannylpyridine-2-carbonyl azide, tetrahydrofuran, 79%; (2) Pd(PPh$_3$)$_4$, 2-bromothiophene, dimethylformamide, 76%; (g) *p*-nitrobenzoyl chloride, triethylamine, CHCl$_3$, 83%; (h) chiral HPLC; (i) LiBH$_4$, MeOH, tetrahydrofuran, 22% (for **21a**), 34% (for **21b**).
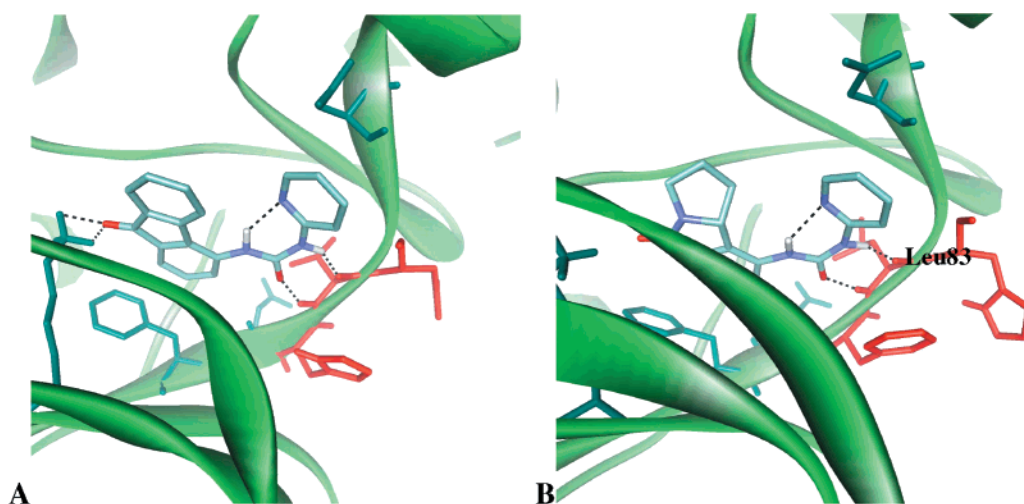
Figure 8. Comparison of modeling prediction and X-ray analysis. **A**: mode A of **15** in the Cdk4 model. **B**: X-ray analysis of the Cdk2−**26a** complex (PDB ID: 1GIH).[38] Green residues: conserved amino acid residues in Cdk4 and Cdk2. Red residues: different amino acid residues in Cdk4 and Cdk2. Broken lines: predicted hydrogen bonds.

of the LEGEND and the SEEDS was so effective that we were able to overcome the difficulty in utilizing output structures from the *de novo* design program and identified some promising scaffolds including diarylurea. Construction of informer libraries, prediction of the binding mode by molecular modeling, and modification based on the predicted binding mode led efficiently to potent lead compounds (0.01 μM order) from initial compounds (10−100 μM order). Recently, high-throughput screening (HTS) has become an essential technique in lead identification. It is expected that it should accelerate assay throughput and reduce assay costs.

However, the success rate of lead discovery for various kinds of drug discovery targets is not supposed to be changed dramatically, because the success rate depends on whether the screening source has sufficient size and structural diversity. When a reliable 3D structure or model of a target protein is available, our methodology of structure-based lead generation would be an alternative approach to development of lead compounds.

The binding mode of **15** in Cdk4 as predicted by molecular modeling was confirmed by SAR and X-ray analysis of the Cdk2−**26a** complex. Compound **26a** showed moderately higher selectivity (>50-fold) over the

other kinases[39] with the exception of the Cdk family. However, **26a** inhibited Cdk1/2 with comparable IC$_{50}$ values (0.120 μM/0.078 μM). As a next step, we designed highly selective Cdk4 inhibitors based on this binding mode and structural information about differences between Cdk4 and other kinases. The results are reported in the following article.

Experimental Section

Materials and Methods. All reagents and solvents were of commercial quality and were used without further purification unless otherwise noted. Melting points were determined with a Yanaco MP micromelting point apparatus (Yanagimoto Seisakusho Co., Japan) and were not corrected. ^{1}H NMR spectra were obtained on a Varian Gemini-300 (300 MHz) or Gemini-200 (200 MHz) with tetramethylsilane as an internal standard. Mass spectrometry was performed with a JEOL JMS-SX 102A (FAB positive) or micromass QUATTRO II (ESI positive). High-resolution mass spectra (HR-MS) were determined in a micromass Q-TOF2 (ESI positive). Optical rotations were measured with a Jasco DIP-370 polarimeter. Thin-layer chromatography (TLC) analysis was performed on Merck Kieselgel F$_{254}$ precoated plates. Silica gel column chromatography was carried out on Wako gel C-300 (Wako Pure Chemicals Industries, Japan).

General Procedure for Preparation of *N*-Alkyl-*N*'-(7-hydroxy-1-naphthyl)urea. To a stirred solution of 1-amino-7-hydroxynaphthalene (1.59 g, 10 mmol) in pyridine (30 mL) was added methyl chloroformate (850 mL, 11 mmol) at 0 °C. After the mixture was stirred for 30 min, methyl chloroformate (430 mL, 5.6 mmol) was added. After being stirred for 15 min, the reaction mixture was poured into water. The aqueous layer was extracted with EtOAc. The combined organic layer was washed successively with 2 N HCl, water, and brine, dried over MgSO$_4$, and concentrated in vacuo. The residue was purified by silica gel column chromatography (EtOAc) to give methyl 7-hydroxy-1-naphthylcarbamate (2.20 g, 100%) as a purple oil. ^{1}H NMR (300 MHz, CDCl$_3$): δ 6.72 (1H, brs), 7.09 (1H, d, J = 9.6 Hz), 7.30 (1H, t, J = 8.0 Hz), 7.63 (1H, d, J = 8.0 Hz), 7.68 (1H, m), 7.73 (1H, d, J = 9.6 Hz). MS (ESI+): m/z 218 (M+H)$^+$. HR-MS calcd for C$_{12}$H$_{12}$NO$_3$ (M+H)$^+$: 218.0817, found 218.0828. A solution of methyl 7-hydroxy-1-naphthylcarbamate (58 mg, 0.27 mmol) in toluene (3 mL) was mixed with triethylamine (82 mL, 0.59 mmol) and refluxed. After 10 min, *B*-chlorocatecholborane (82 mg, 0.53 mmol) was added. After 15 min, 1.2 equiv of amine was added and refluxed for 10 min. The reaction mixture was poured into water. The aqueous layer was extracted with EtOAc. The combined organic layer was washed successively with saturated aqueous NaHCO$_3$ and brine, dried over MgSO$_4$, and concentrated in vacuo. The residue was purified by silica gel column chromatography to give *N*-alkyl-*N*'-(7-hydroxy-1-naphthyl)urea. Yields ranged from 30 to 70%.

The following compounds (**1a**, **1b**, **1c**, **1d**, **1e**, **1f**, **1g**, and **14**) were synthesized from the appropriate amines and methyl 7-hydroxy-1-naphthylcarbamate by this method.

N-(7-Hydroxy-1-naphthyl)-N'-phenylurea (1a). ^{1}H NMR (200 MHz, DMSO-d_6): δ 6.96 (1H, t, J = 6.8 Hz), 7.12 (1H, dd, J_1 = 8.9, J_2 = 1.6 Hz), 7.24 (1H, d, J = 6.8 Hz), 7.30 (2H, d, J = 7.9 Hz), 7.33 (1H, m), 7.47 (2H, d, J = 7.9 Hz), 7.51 (1H, m), 7.78 (2H, t, J = 8.9 Hz), 8.46 (1H, s), 9.00 (1H, s), 9.98 (1H, s). MS (FAB+): m/z 279 (M+H)$^+$. HR-MS calcd for C$_{17}$H$_{15}$N$_2$O$_2$ (M+H)$^+$: 279.1134, found 279.1132.

N-(7-Hydroxy-1-naphthyl)-N'-pyridin-3-ylurea (1b). ^{1}H NMR (300 MHz, DMSO-d_6): δ 7.10 (1H, d, J = 6.7 Hz), 7.22 (1H, t, J = 7.8 Hz), 7.33 (2H, m), 7.55 (1H, d, J = 7.8 Hz), 7.98 (1H, d, J = 6.7 Hz), 8.18 (1H, d, J = 5.6 Hz), 8.60 (2H, d, J = 9.6 Hz), 9.14 (1H, s), 9.80 (1H, s). MS (FAB+): m/z 280 (M+H)$^+$. HR-MS calcd for C$_{16}$H$_{14}$N$_3$O$_2$ (M+H)$^+$: 280.1086, found 280.1091.

N-(7-Hydroxy-1-naphthyl)-N'-pyridin-4-ylurea (1c). ^{1}H NMR (300 MHz, DMSO-d_6): δ 7.11 (1H, d, J = 6.7 Hz), 7.23 (1H, t, J = 7.8 Hz), 7.30 (1H, s), 7.46 (2H, d, J = 5.6 Hz), 7.57 (1H, d, J = 9.6 Hz), 7.76 (2H, t, J = 9.6 Hz), 8.36 (2H, d, J = 5.6 Hz), 8.64 (1H, s), 9.39 (1H, s), 9.80 (1H, s). MS (FAB+): m/z 280 (M+H)$^+$. HR-MS calcd for C$_{16}$H$_{14}$N$_3$O$_2$ (M+H)$^+$: 280.1086, found 280.1092.

N-(7-Hydroxy-1-naphthyl)-N'-(1,3-thiazol-2-yl)urea (1d). ^{1}H NMR (300 MHz, DMSO-d_6): δ 7.13 (2H, m), 7.24 (1H, t, J = 7.8 Hz), 7.28 (1H, s), 7.39 (1H, d, J = 5.6 Hz), 7.57 (1H, d, J = 9.6 Hz), 7.78 (2H, t, J = 9.6 Hz), 7.83 (1H, d, J = 5.6 Hz), 8.89 (1H, s), 9.84 (1H, s), 10.77 (1H, s). MS (FAB+): m/z 286 (M+H)$^+$. HR-MS calcd for C$_{14}$H$_{12}$N$_3$O$_2$S (M+H)$^+$: 286.0650, found 286.0650.

N-Benzyl-N'-(7-hydroxy-1-naphthyl)urea (1e). ^{1}H NMR (300 MHz, DMSO-d_6): δ 4.34 (2H, d, J = 5.6 Hz), 6.94 (1H, t, J = 5.6 Hz), 7.08 (1H, d, J = 6.7 Hz), 7.16 (1H, t, J = 7.8 Hz), 7.21−7.38 (6H, m), 7.44 (1H, d, J = 7.8 Hz), 7.72 (1H, d, J = 9.6 Hz), 7.80 (1H, t, J = 7.8 Hz), 8.32 (1H, s), 9.73 (1H, s). MS (FAB+): m/z 293 (M+H)$^+$. HR-MS calcd for C$_{18}$H$_{17}$N$_2$O$_2$ (M+H)$^+$: 293.1290, found 293.1293.

N-(7-Hydroxy-1-naphthyl)-N'-isopropylurea (1f). ^{1}H NMR (200 MHz, DMSO-d_6): δ 1.12 (6H, d, J = 7.2 Hz), 3.77 (1H, heptet, J = 7.2 Hz) 6.38 (1H, d, J = 7.5 Hz), 7.07 (1H, d, J = 8.6 Hz), 7.16 (1H, d, J = 7.5 Hz), 7.28 (1H, s), 7.42 (1H, d, J = 7.5 Hz), 7.72 (1H, d, J = 8.6 Hz), 7.80 (1H, d, J = 7.5 Hz), 8.07 (1H, s), 9.69 (1H, s). MS (FAB+): m/z 245 (M+H)$^+$. HR-MS calcd for C$_{14}$H$_{17}$N$_2$O$_2$ (M+H)$^+$: 245.1290, found 245.1298.

N-Cyclopentyl-N'-(7-hydroxy-1-naphthyl)urea (1g). ^{1}H NMR (300 MHz, DMSO-d_6): δ 1.33−1.92 (8H, m), 3.98(1H, m) 6.55 (1H, d, J = 7.7 Hz), 7.08 (1H, d, J = 9.0 Hz), 7.14 (1H, t, J = 7.7 Hz), 7.28 (1H, s), 7.40 (1H, d, J = 7.7 Hz), 7.72 (1H, d, J = 9.0 Hz), 7.82 (1H, d, J = 7.7 Hz), 8.06 (1H, s), 9.69 (1H, s). MS (FAB+): m/z 271 (M+H)$^+$. HR-MS calcd for C$_{16}$H$_{19}$N$_2$O$_2$ (M+H)$^+$: 271.1447, found 271.1439.

N-(7-Hydroxy-1-naphthyl)-N'-pyridin-2-ylurea (14). mp 224−225 °C. ^{1}H NMR (300 MHz, DMSO-d_6): δ 7.06 (1H, t, J = 5.6 Hz), 7.12 (1H, d, J = 6.7 Hz), 7.24 (1H, t, J = 7.8 Hz), 7.37 (2H, m), 7.55 (1H, d, J = 7.8 Hz), 7.78 (2H, m), 8.00 (1H, d, J = 6.7 Hz), 8.40 (1H, d, J = 5.6 Hz), 9.82 (1H, s), 9.88 (1H, s), 11.18 (1H, brs). MS (FAB+): m/z 280 (M+H)$^+$. HR-MS calcd for C$_{16}$H$_{14}$N$_3$O$_2$ (M+H)$^+$: 280.1086, found 280.1088. Anal. (C$_{16}$H$_{13}$N$_3$O$_2$·0.33H$_2$O) C, H, N.

N-(7-Hydroxy-1-naphthyl)-2-phenylacetamide (13). To a stirred solution of 1-amino-7-hydroxynaphthalene (159 mg, 1.0 mmol) in tetrahydrofuran (10 mL) were added phenylacetic acid (164 mg, 1.0 mmol) and dicyclohexyl carbodiimide (250 mg, 1.2 mmol), and the resultant mixture was stirred at room temperature for 10 h. The reaction mixture was concentrated in vacuo. The residue was purified by silica gel column chromatography (hexane−EtOAc (2:1)) and precipitated with EtOAc to give **13** (214 mg, 77%). ^{1}H NMR (200 MHz, DMSO-d_6): δ 3.77 (2H, s), 7.10 (1H, d, J = 8.2 Hz), 7.17−7.44 (7H, m), 7.48 (1H, d, J = 8.2 Hz), 7.61 (1H, d, J = 8.2 Hz), 7.76 (1H, d, J = 9.4 Hz), 9.79 (1H, s), 9.95 (1H, s). MS (FAB+): m/z 278 (M+H)$^+$. HR-MS calcd for C$_{18}$H$_{16}$NO$_2$ (M+H)$^+$: 278.1181, found 278.1183.

General Procedure for Preparation of *N*-Alkyl-*N*'-pyridin-2-ylurea. To a stirred solution of thionyl chloride (10 mL) was added picolinic acid (2.47 g, 20 mmol) with heating at 85 °C for 1 h. The reaction mixture was evaporated to afford crude picolinic chloride as a dark purple solid. The crude picolinic chloride was dissolved in water (20 mL) at 0 °C. Sodium azide (1.84 g, 28 mmol) was added, and the resultant mixture was stirred at room temperature for 15 min and poured into saturated aqueous NaHCO$_3$. The aqueous layer was extracted with EtOAc. The combined organic layer was washed with brine, dried over MgSO$_4$, and concentrated in vacuo. The residue was purified by rapid silica gel column chromatography (hexane−EtOAc (1:1)) to yield pyridine-2-carbonyl azide (1.06 g, 34%). ^{1}H NMR (300 MHz, DMSO-d_6): δ 7.55 (1H, dd, J_1 = 9.0 Hz, J_2 = 6.7 Hz), 7.88 (1H, t, J = 9.0 Hz), 8.17 (1H, d, J = 9.0 Hz), 8.77 (1H, d, J = 6.7 Hz). MS (ESI+): m/z 149 (M+H)$^+$. A solution of pyridine-2-carbonyl azide (25 mg, 0.17 mmol) in tetrahydrofuran (2 mL) was heated at 85 °C. After 30 min, 1.0 equiv of amine was added, and the

resultant mixture was stirred for 2 h at the same temperature. The reaction mixture was evaporated, and the residue was precipitated from hexane−EtOAc (1:1) to give *N*-alkyl-*N*-pyridin-2-ylurea. Yields ranged from 10 to 70%.

The following compounds (**14a**, **14b**, **14c**, **14d**, **14e**, **14f**, **15**, **25**, **26a**, **26b**, **27**, and **28**) were prepared from the appropriate amines and pyridine-2-carbonyl azide by this procedure.

N-(1H-Indazol-6-yl)-N-pyridin-2-ylurea (14a). mp 220−221 °C. ^{1}H NMR (300 MHz, DMSO-d_6): δ 6.95−6.99 (2H, m), 7.48 (1H, d, J = 8.2 Hz), 7.66 (1H, d, J = 8.2 Hz), 7.75 (1H, t, J = 8.2 Hz), 7.95 (1H, s), 8.06 (1H, s), 8.30 (1H, d, J = 4.7 Hz), 9.49 (1H, s), 10.73 (1h, brs). MS (ESI+): m/z 254 (M+H)$^+$. HR-MS calcd for $C_{13}H_{12}N_5O$ (M+H)$^+$: 254.1042, found 254.1065. Anal. ($C_{13}H_{11}N_5O\cdot0.25H_2O$) C, H, N.

N-Pyridin-2-yl-N-quinolin-5-ylurea (14b). mp 213-215 °C. ^{1}H NMR (300 MHz, DMSO-d_6): δ 7.06 (1H, dd, J_1 = 7.3 Hz, J_1 = 5.1 Hz), 7.42 (1H, d, J = 8.2 Hz), 7.64−7.71 (1H, m), 7.73−7.83 (3H, m), 8.23 (1H, dd, J_1 = 6.7 Hz, J_1 = 2.1 Hz), 8.41 (1H, dd, J_1 = 5.1 Hz, J_1 = 2.1 Hz), 8.54 (1H, d, J = 8.8 Hz), 8.95 (1H, dd, J_1 = 4.1 Hz, J_1 = 1.4 Hz), 9.88 (1H, s), 11.41 (1H, brs). MS (ESI+): m/z 265 (M+H)$^+$. HR-MS calcd for $C_{15}H_{13}N_4O$ (M+H)$^+$: 265.1089, found 265.1096. Anal. ($C_{15}H_{12}N_4O$) C, H, N.

N-(1,3-Dioxo-2,3-dihydro-1H-isoindol-4-yl)-N-pyridin-2-ylurea (14c). mp >300 °C. ^{1}H NMR (300 MHz, DMSO-d_6): δ 7.04−7.10 (1H, m), 7.19 (1H, d, J = 8.3 Hz), 7.41 (1H, d, J = 6.9 Hz), 7.71−7.82 (2H, m), 8.35 (1H, dd, J_1 = 4.9 Hz, J_1 = 1.6 Hz), 8.74 (1H, d, J = 8.3 Hz), 10.19 (1H, s), 11.29 (1H, s), 12.57 (1H, brs). MS (ESI+): m/z 283 (M+H)$^+$. HR-MS calcd for $C_{14}H_{11}N_4O_3$ (M+H)$^+$: 283.0831, found 283.0822. Anal. ($C_{14}H_{10}N_4O_3$) C, H, N.

N-Phenyl-N-pyridin-2-ylurea (14d). mp 186−188 °C. ^{1}H NMR (300 MHz, DMSO-d_6): δ 6.97−7.04 (2H, m), 7.30 (1H, d, J = 7.4 Hz), 7.46−7.53 (3H, m), 7.71−7.76 (1H, m), 8.27 (1H, dd, J_1 = 5.0 Hz, J_1 = 1.9 Hz), 9.41 (1H, s), 10.48 (1H, s). MS (ESI+): m/z 214. (M+H)$^+$. HR-MS calcd for $C_{12}H_{12}N_3O$ (M+H)$^+$: 214.0980, found 214.0977. Anal. ($C_{12}H_{11}N_3O$) C, H, N.

N-Benxyl-N-pyridin-2-ylurea (14e). mp 143−145 °C. ^{1}H NMR (300 MHz, CDCl$_3$): δ 4.63 (1H, d, J = 5.9 Hz), 6.79 (1H, d, J = 8.2 Hz), 6.83−6.87 (1H, m), 7.23−7.41 (5H, m), 7.56 (1H, t, J = 8.2 Hz), 8.12 (1H, d, J = 4.1 Hz), 8.60 (1H, s), 9.83 (1H, br). MS (ESI+): m/z 228. (M+H)$^+$. HR-MS calcd for $C_{13}H_{14}N_3O$ (M+H)$^+$: 228.1137, found 228.1135. Anal. ($C_{13}H_{13}N_3O\cdot0.1H_2O$) C, H, N.

N-Cyclohexyl-N-pyridin-2-ylurea (14f). mp 122−123 °C. ^{1}H NMR (300 MHz, CDCl$_3$): δ 1.26−1.51 (5H, m), 1.59−1.79 (3H, m), 2.00−2.06 (2H, m), 3.82−3.86 (1H, m), 6.82 (1H, d, J = 8.4 Hz), 6.84−6.88 (1H, m), 7.58 (1H, t, J = 8.4 Hz), 8.18 (1H, dd, J_1 = 5.1 Hz, J_1 = 1.1 Hz), 8.27 (1H, brs), 9.32 (1H, m). MS (ESI+): m/z 220. (M+H)$^+$. HR-MS calcd for $C_{12}H_{18}N_3O$ (M+H)$^+$: 220.150, found 220.1450. Anal. ($C_{12}H_{17}N_3O$) C, H, N.

N-(9-Oxo-9H-fluoren-4-yl)-N-pyridin-2-ylurea (15). mp >300 °C. ^{1}H NMR (300 MHz, DMSO-d_6): δ 7.07 (1H, dd, J_1 = 8.3 Hz, J_2 = 5.1 Hz), 7.34−7.45 (4H, m), 7.64−7.69 (2H, m), 7.78−7.84 (1H, m), 8.04 (1H, d, J = 7.9 Hz), 8.08 (1H, d, J = 7.7 Hz), 8.29 (1H, dd, J_1 = 5.0 Hz, J_2 = 1.2 Hz), 10.03 (1H, s), 11.12 (1H, brs). MS (FAB+): m/z 316 (M+H)$^+$. HR-MS calcd for $C_{19}H_{14}N_3O_2$ (M+H)$^+$: 316.1086, found 316.1084. Anal. ($C_{19}H_{13}N_3O_2$) C, H, N.

N-(5-Oxo-5H-pyrrolo[2,1-a]isoindol-9-yl)-N-pyridin-2-ylurea (25). mp 268−269 °C. ^{1}H NMR (300 MHz, DMSO-d_6): δ 6.34 (1H, t, J = 3.1 Hz), 6.65 (1H, d, J = 3.1 Hz), 7.08 (1H, dd, J_1 = 6.7 Hz, J_2 = 5.6 Hz), 7.24−7.29 (3H, m), 7.38 (1H, d, J = 7.3 Hz), 7.77−7.83 (1H, m), 8.27 (1H, d, J = 8.2 Hz), 8.31 (1H, dd, J_1 = 5.1 Hz, J_2 = 1.1 Hz), 10.06 (1H, s), 10.97 (1H, brs). MS (FAB+): m/z 305 (M+H)$^+$. HR-MS calcd for $C_{17}H_{13}N_4O_2$ (M+H)$^+$: 305.1039, found 305.1035.

N-[(9bR)-5-Oxo-2,3,5,9b-tetrahydro-1H-pyrrolo[2,1-a]isoindol-9-yl]-N-pyridin-2-ylurea (26a). mp 213−215 °C. ^{1}H NMR (300 MHz, DMSO-d_6): δ 1.06−1.20 (1H, m), 2.30−2.43 (2H, m), 2.52−2.57 (1H, m), 3.28−3.35 (1H, m), 3.50−3.60 (1H, m), 4.83 (1H, dd, J_1 = 10.0 Hz, J_2 = 5.7 Hz), 7.06 (1H, dd, J_1

= 7.2 Hz, J_2 = 5.1 Hz), 7.28−7.33 (2H, m), 7.46 (1H, t, J = 7.7 Hz), 7.76−7.82 (1H, m), 8.29−8.32 (2H, m), 9.95 (1H, s), 11.19 (1H, brs). MS (FAB+): m/z 309 (M+H)$^+$. HR-MS calcd for $C_{17}H_{17}N_4O_2$ (M+H)$^+$: 309.1352, found 309.1353. [α]$_D^{20}$ 162.0° (c 1.0, CHCl$_3$). Anal. ($C_{17}H_{16}N_4O_2\cdot0.33H_2O$) C, H, N.

N-[(9bS)-5-Oxo-2,3,5,9b-tetrahydro-1H-pyrrolo[2,1-a]isoindol-9-yl]-N-pyridin-2-ylurea (26b). mp 213−215 °C. ^{1}H NMR (300 MHz, DMSO-d_6): δ 1.06−1.20 (1H, m), 2.30−2.43 (2H, m), 2.52−2.57 (1H, m), 3.28−3.35 (1H, m), 3.50−3.60 (1H, m), 4.83 (1H, dd, J_1 = 10.0 Hz, J_2 = 5.7 Hz), 7.06 (1H, dd, J_1 = 7.2 Hz, J_2 = 5.1 Hz), 7.28−7.33 (2H, m), 7.46 (1H, t, J = 7.7 Hz), 7.76−7.82 (1H, m), 8.29−8.32 (2H, m), 9.95 (1H, s), 11.19 (1H, brs). MS (FAB+): m/z 309 (M+H)$^+$. HR-MS calcd for $C_{17}H_{17}N_4O_2$ (M+H)$^+$: 309.1352, found 309.1351. [α]$_D^{20}$ −156.0° (c 1.0, CHCl$_3$). Anal. ($C_{17}H_{16}N_4O_2\cdot0.2H_2O$) C, H, N.

N-(3-(1-Hydroxyvinyl)-5-oxo-5H-pyrrolo[2,1-a]isoindol-9-yl)-N-pyridin-2-ylurea (27). mp >300 °C. ^{1}H NMR (300 MHz, DMSO-d_6): δ 6.32−6.35 (1H, m), 6.74 (1H, s), 7.07 (1H, dd, J_1 = 7.2 Hz, J_2 = 5.2 Hz), 7.19 (1H, s), 7.26 (1H, s), 7.40 (1H, t, J = 8.0 Hz), 7.47 (1H, d, J = 8.6 Hz), 7.66 (1H, dd, J_1 = 7.9 Hz, J_2 = 1.5 Hz), 7.78−7.83 (1H, m), 8.25 (1H, dd, J_1 = 5.2 Hz, J_2 = 1.6 Hz), 8.47 (1H, dd, J_1 = 8.0 Hz, J_2 = 1.6 Hz), 10.06 (1H, s), 10.85 (1H, brs), 11.96 (1H, s). MS (FAB+): m/z 347 (M+H)$^+$. HR-MS calcd for $C_{19}H_{15}N_4O_3$ (M+H)$^+$: 347.1144, found 347.1149.

N-(5-Oxo-2,3,5,9b-tetrahydro-1H-pyrrolo[2,1-a]isoindol-9-yl)-N-(4-thien-2-ylpyridin-2-yl)urea (28). A solution of 4-(tributylstannyl)pyridine-2-carbonyl azide (300 mg, 0.69 mmol) in tetrahydrofuran (10 mL) was heated at 85 °C. After 30 min, **21** (150 mg, 0.79 mmol) was added, and the resultant mixture was stirred for 2 h at the same temperature. The reaction mixture was evaporated, and the residue was precipitated from hexane−EtOAc (1:1) to yield *N*-(5-oxo-2,3,5,9b-tetrahydo-1*H*-pyrrolo[2,1-*a*]isoindol-9-yl)-*N*-[4-(tributylstannyl)pyridin-2-yl]urea (326 mg, 79%). mp 149−150 °C. ^{1}H NMR (300 MHz, CDCl$_3$): δ 0.89 (9H, t, J = 8.0 Hz), 1.04−1.20 (1H, m), 1.10−1.15 (6H, m), 1.27−1.36 (6H, m), 1.51−1.58 (6H, m), 2.40−2.48 (2H, m), 2.64−2.68 (1H, m), 3.46−3.50 (1H, m), 3.75−3.79 (1H, m), 4.80 (1H, dd, J_1 = 10.5 Hz, J_2 = 5.5 Hz), 6.92 (1H, s), 7.07 (1H, d, J = 4.9 Hz), 7.47 (1H, t, J = 7.9 Hz), 7.53 (1H, d, J = 7.9 Hz), 8.01 (1H, brs), 8.09 (1H, d, J = 4.9 Hz), 8.36 (1H, d, J = 7.9 Hz), 12.07 (1H, brs). HR-MS calcd for $C_{29}H_{43}N_4O_2{}^{120}$Sn (M+H)$^+$: 599.2408, found 599.2418. To a solution of *N*-(5-oxo-2,3,5,9b-tetrahydo-1*H*-pyrrolo[2,1,-*a*]isoindol-9-yl)-*N*-[4-(tributylstannyl)pyridin-2-yl]urea (200 mg, 0.34 mmol) in dimethylformamide (15 mL) were added 2-bromothiophene (164 mg, 1.0 mmol) and tetrakis-(triphenylphosphin)palladium (100 mg, 0.086 mmol). The resultant mixture was stirred for 10 h at 110 °C, and poured into water. The aqueous layer was extracted with EtOAc. The combined organic layer was washed successively with saturated aqueous NH$_4$Cl, water, and brine, dried over MgSO$_4$, and concentrated in vacuo. The residue was purified by silica gel column chromatography (3% MeOH in CHCl$_3$) and precipitated from EtOAc−Et$_2$O to provide **28** (102 mg, 76%) as a white solid. mp 245−247 °C. ^{1}H NMR (300 MHz, DMSO-d_6): δ 1.08−1.20 (1H, m), 2.26−2.45 (2H, m), 2.48−2.61 (1H, m), 3.29−3.39 (1H, m), 3.49−3.59 (1H, m), 4.80−4.88 (1H, m), 7.23 (1H, t, J = 4.0 Hz), 7.32 (1H, d, J = 6.6 Hz), 7.38 (1H, d, J = 4.0 Hz), 7.47 (1H, t, J = 6.6 Hz), 7.59 (1H, brs), 7.70−7.76 (2H, m), 8.30 (2H, d, J = 6.6 Hz), 9.97 (1H, s), 11.03 (1H, br). HR-MS calcd for $C_{21}H_{19}N_4O_2S$ (M+H)$^+$: 391.1229, found 391.1228.

1-(2-Bromo-3-nitrobenzoyl)-1H-pyrrole (17). To a stirred solution of thionyl chloride (20 mL) was added 2-bromo-3-nitrobenzoic acid (2.0 g, 8.1 mmol), and the resultant mixture was heated at 80 °C for 3 h. After cooling to room temperature, the reaction mixture was concentrated in vacuo. The residue was dissolved in dichloromethane (20 mL). Then pyrrole (2.3 mL, 33 mmol) and triethylamine (5 mL, 36 mmol) were added. The reaction mixture was stirred at room temperature for 10 h and poured into water. The aqueous layer was extracted with EtOAc. The combined organic layer was washed successively

with saturated aqueous NH_4Cl, water, and brine, dried over $MgSO_4$, and concentrated in vacuo. The residue was purified by silica gel column chromatography (hexane−EtOAc (2:1)) to afford **17** (865 mg, 36%) as a colorless oil. ^{1}H NMR (300 MHz, $CDCl_3$): δ 6.26 (1H, d, J = 2.0 Hz), 6.38 (2H, t, J = 2.3 Hz), 6.83 (1H, d, J = 2.1 Hz), 7.63 (2H, d, J = 5.0 Hz), 7.93 (1H, d, J = 4.9 Hz). MS (ESI+): m/z 296 (M+H)[+].

2-Acetyl-1-(2-bromo-3-nitrobenzoyl)-1*H*-pyrrole (18). To a stirred solution of thionyl chloride (30 mL) was added 2-bromo-3-nitrobenzoic acid (10 g, 41 mmol), and the resultant mixture was heated at 80 °C for 3 h. After cooling to room temperature, the reaction mixture was evaporated. The residue was dissolved in dichloromethane (100 mL). Then 2-acetylpyrrole (8.9 g, 81 mmol) and triethylamine (20 mL, 163 mmol) were added. The resultant mixture was stirred at room temperature for 10 h, and poured into water. The aqueous layer was extracted with EtOAc. The combined organic layer was washed successively with saturated aqueous NH_4Cl, water, and brine, dried over $MgSO_4$, and concentrated in vacuo. The residue was purified by precipitation from hexane−$CHCl_3$ (2:1) to give **18** (9.2 g, 67%) as a white solid. mp 170−172 °C. ^{1}H NMR (300 MHz, $CDCl_3$): δ 2.0.27 (3H, s), 6.47 (1H, t, J = 3.3 Hz), 7.38 (1H, d, J = 3.3 Hz), 7.49 (1H, d, J = 7.9 Hz), 7.61−7.68 (2H, m), 8.11 (1H, d, J = 7.9 Hz). MS (ESI+): m/z 336 (M+H)[+]. HR-MS calcd for $C_{13}H_{10}N_2O_4{}^{79}Br$ (M+H)[+]: 336.9824, found 336.9835.

9-Nitro-5*H*-pyrrolo[2,1-*a*]isoindol-5-one (19). To a stirred solution of **17** (865 mg, 2.9 mmol) in dimethylacetamide (20 mL) were added potassium acetate (575 mg, 6.0 mmol) and tetrakis(triphenylphosphin)palladium (100 mg, 0.086 mmol), and the resultant mixture was heated at 130 °C for 10 h. After cooling to room temperature, the reaction mixture was poured into water. The aqueous layer was extracted with EtOAc. The combined organic layer was washed successively with water and brine, dried over $MgSO_4$, and concentrated in vacuo. The residue was purified by silica gel column chromatography (hexane−EtOAc (5:1)) to yield **19** (509 mg, 81%) as a red solid. mp 152−153 °C. ^{1}H NMR (300 MHz, $CDCl_3$): δ 6.33 (1H, t, J = 3.2 Hz), 7.08 (1H, d, J = 3.2 Hz), 7.19 (1H, d, J = 3.2 Hz), 7.35 (1H, t, J = 8.3 Hz), 7.92 (1H, d, J = 8.3 Hz), 8.27 (1H, d, J = 8.3 Hz). MS (ESI+): m/z 215 (M+H)[+].

3-(1-Hydroxyvinyl)-9-nitro-5*H*-pyrrolo[2,1-*a*]isoindol-5-one (20). To a stirred solution of **18** (2.0 g, 5.9 mmol) in dimethylacetamide (40 mL) were added potassium acetate (1.16 g, 12 mmol) and tetrakis(triphenylphosphin)palladium (700 mg, 0.61 mmol), and the resultant mixture was heated at 110 °C for 2 h. After cooling to room temperature, the reaction mixture was poured into water. The aqueous layer was extracted with EtOAc. The combined organic layer was washed successively with water and brine, dried over $MgSO_4$, and concentrated in vacuo. The residue was purified by silica gel column chromatography (hexane−EtOAc (2:1)) to yield **20** (941 mg, 62%) as a yellow solid. mp 208−210 °C. ^{1}H NMR (300 MHz, DMSO-d_6): δ 6.33−6.36 (1H, m), 6.81 (1H, s), 6.94−6.97 (1H, m), 7.25−7.27 (1H, m), 7.61 (1H, t, J = 7.9 Hz), 8.32 (1H, d, J = 7.9 Hz), 8.45 (1H, d, J = 7.9 Hz), 12.00 (1H, brs). MS (ESI+): m/z 257 (M+H)[+]. HR-MS calcd for $C_{13}H_9N_2O_4$ (M+H)[+]: 257.0562, found 257.0560.

9-Amino-1,2,3,9b-tetrahydro-5*H*-pyrrolo[2,1-*a*]isoindol-5-one (21). To a stirred solution of **19** (50 mg, 0.23 mmol) in MeOH (10 mL) was added 10% Pd/C (25 mg), and the mixture was stirred at room temperature for 2 h under an atmospheric pressure of hydrogen. The catalyst was removed by filtration, and the filtrate was evaporated to yield racemate **21** (48 mg, 99%) as a white solid. mp 149−152 °C. ^{1}H NMR (300 MHz, DMSO-d_6): δ 0.80−0.93 (1H, m), 2.10−2.30 (2H, m), 2.43−2.51 (1H, m), 3.18−3.24 (1H, m), 3.38−3.47 (1H, m), 4.50 (1H, dd, J_1 = 10.0 Hz, J_1 = 5.5 Hz), 5.34 (2H, s), 6.72 (1H, d, J = 7.9 Hz), 6.76 (1H, d, J = 7.9 Hz), 7.11 (1H, t, J = 7.9 Hz). MS (ESI+): m/z 189 (M+H)[+]. HR-MS calcd for $C_{11}H_{13}N_2O$ (M+H)[+]: 189.1028, found 189.1025.

4-Nitro-*N*-(5-oxo-2,3,5,9b-tetrahydro-1*H*-pyrrolo[2,1-*a*]-isoindol-9-yl)benzamide (22). To a stirred solution of **21** (30 mg, 0.16 mmol) in $CHCl_3$ (10 mL) were added triethylamine

(44 mL, 0.32 mmol) and *p*-nitrobenzoyl chloride (59 mg, 0.32 mmol). After being stirred for 3 h, the reaction mixture was poured into a saturated $NaHCO_3$ solution. The aqueous layer was extracted with $CHCl_3$. The combined organic layer was washed with brine, dried over $MgSO_4$, and concentrated in vacuo. The residue was purified by silica gel column chromatography (2% MeOH in $CHCl_3$) to give racemate **22** (45 mg, 83%) as a slight yellow foam. ^{1}H NMR (300 MHz, $CDCl_3$): δ 1.25−1.31 (1H, m), 2.20−2.27 (1H, m), 2.33−2.42 (2H, m), 3.42−3.47 (1H, m), 3.68−3.72 (1H, m), 4.92 (1H, dd, J_1 = 11.2 Hz, J_2 = 5.9 Hz), 7.53 (1H, d, J = 7.8 Hz), 7.68 (1H, t, J = 7.8 Hz), 7.82 (1H, d, J = 7.8 Hz), 8.12 (2H, d, J = 8.8 Hz), 8.22 (1H, brs), 8.38 (2H, d, J = 8.8 Hz). HR-MS calcd for $C_{18}H_{16}N_3O_4$ (M+H)[+]: 338.1141, found 338.1134.

N-[(9b*R*)-5-Oxo-2,3,5,9b-tetrahydro-1*H*-pyrrolo[2,1-*a*]isoindol-9-yl]-4-nitrobenzamide (22a) and *N*-[(9b*S*)-5-Oxo-2,3,5,9b-tetrahydro-1*H*-pyrrolo[2,1-*a*]isoindol-9-yl]-4-nitrobenzamide (22b). Compound **22** (22 g, 66 mmol) was separated by chiral HPLC (CHIRALPAK AD, $50\phi \times 500$ mm, hexane−EtOH (1:4), flow rate 100 mL/min) to give **22a** (retention time: 30 min, 10.1 g) and **22b** (retention time: 22 min, 11.2 g) as pale yellow foams. **22a:** ^{1}H NMR (300 MHz, $CDCl_3$): δ 1.25−1.31 (1H, m), 2.20−2.27 (1H, m), 2.33−2.42 (2H, m), 3.42−3.47 (1H, m), 3.68−3.72 (1H, m), 4.92 (1H, dd, J_1 = 11.2 Hz, J_2 = 5.9 Hz), 7.53 (1H, d, J = 7.8 Hz), 7.68 (1H, t, J = 7.8 Hz), 7.82 (1H, d, J = 7.8 Hz), 8.12 (2H, d, J = 8.8 Hz), 8.22 (1H, brs), 8.38 (2H, d, J = 8.8 Hz). HR-MS calcd for $C_{18}H_{16}N_3O_4$ (M+H)[+]: 338.1141, found 338.1135. [α]$_D^{20}$ 134.4° (*c* 1.0, $CHCl_3$). **22b:** ^{1}H NMR (300 MHz, $CDCl_3$): δ 1.25−1.31 (1H, m), 2.20−2.27 (1H, m), 2.33−2.42 (2H, m), 3.42−3.47 (1H, m), 3.68−3.72 (1H, m), 4.92 (1H, dd, J_1 = 11.2 Hz, J_2 = 5.9 Hz), 7.53 (1H, d, J = 7.8 Hz), 7.68 (1H, t, J = 7.8 Hz), 7.82 (1H, d, J = 7.8 Hz), 8.12 (2H, d, J = 8.8 Hz), 8.22 (1H, brs), 8.38 (2H, d, J = 8.8 Hz). HR-MS calcd for $C_{18}H_{16}N_3O_4$ (M+H)[+]: 338.1141, found 338.1128. [α]$_D^{20}$ −132.8° (*c* 1.0, $CHCl_3$).

(9b*R*)-9-Amino-1,2,3,9b-tetrahydro-5*H*-pyrrolo[2,1-*a*]isoindol-5-one (21a). To a stirred solution of **22a** (10.0 g, 29.6 mmol) in tetrahydrofuran (300 mL) was added lithium borohydride (3.86 g, 177 mmol) at room temperature. Then MeOH (9.7 mL, 237 mmol) in tetrahydrofuran (10 mL) was added in a dropwise manner. The resultant mixture was stirred for 5 h at room temperature and poured into 3 N HCl. The aqueous layer was neutralized with saturated aqueous $NaHCO_3$ and extracted with $CHCl_3$. The combined organic layer was washed with brine, dried over $MgSO_4$, and concentrated in vacuo. The residue was purified by silica gel column chromatography (2% MeOH in $CHCl_3$) and recrystallized from EtOAc to give **21a** (1.2 g, 22%, 100% ee). mp 151−152 °C. ^{1}H NMR (300 MHz, DMSO-d_6): δ 0.80−0.93 (1H, m), 2.10−2.30 (2H, m), 2.43−2.51 (1H, m), 3.18−3.24 (1H, m), 3.38−3.47 (1H, m), 4.50 (1H, dd, J_1 = 10.0 Hz, J_1 = 5.5 Hz), 5.34 (2H, s), 6.72 (1H, d, J = 7.9 Hz), 6.76 (1H, d, J = 7.9 Hz), 7.11 (1H, t, J = 7.9 Hz). HR-MS calcd for $C_{11}H_{13}N_2O$ (M+H)[+]: 189.1028, found 189.1027. [α]$_D^{20}$ 87.6° (*c* 1.0, $CHCl_3$).

(9b*S*)-9-Amino-1,2,3,9b-tetrahydro-5*H*-pyrrolo[2,1-*a*]isoindol-5-one (21b). To a stirred solution of **22b** (11.0 g, 32.6 mmol) in tetrahydrofuran (300 mL) was added lithium borohydride (4.25 g, 195 mmol) at room temperature. Then MeOH (16.0 mL, 391 mmol) in tetrahydrofuran (10 mL) was added in a dropwise manner. The resultant mixture was stirred for 5 h at room temperature and poured into 3 N HCl. The aqueous layer was neutralized with saturated aqueous $NaHCO_3$ and extracted with $CHCl_3$. The combined organic layer was washed with brine, dried over $MgSO_4$, and concentrated in vacuo. The residue was purified by silica gel column chromatography (2% MeOH in $CHCl_3$) and recrystallized from EtOAc to give **21a** (2.1 g, 34%, 100% ee). mp 151−152 °C. ^{1}H NMR (300 MHz, DMSO-d_6): δ 0.80−0.93 (1H, m), 2.10−2.30 (2H, m), 2.43−2.51 (1H, m), 3.18−3.24 (1H, m), 3.38−3.47 (1H, m), 4.50 (1H, dd, J_1 = 10.0 Hz, J_1 = 5.5 Hz), 5.34 (2H, s), 6.72 (1H, d, J = 7.9 Hz), 6.76 (1H, d, J = 7.9 Hz), 7.11 (1H, t, J = 7.9 Hz). HR-MS calcd for $C_{11}H_{13}N_2O$ (M+H)[+]: 189.1028, found 189.1034. [α]$_D^{20}$−87.0° (*c* 1.0, $CHCl_3$).

(1S,4R)-N-[(9bS)-5-Oxo-2,3,5,9b-tetrahydro-1H-pyrrolo-[2,1-a]isoindol-9-yl]-4,7,7-trimethyl-3-oxo-2-oxabicyclo-[2,2,1]heptane-1-carboxamide. To a stirred solution of **21b** (54 mg, 0.29 mmol) in CH_2Cl_2 were added (1S)-(−)-camphanic chloride (126 mg, 0.58 mmol), triethylamine (80 μL, 0.57 mmol), and 4-(dimethylamino)pyridine (3.5 mg, 0.029 mmol). The resultant mixture was stirred for 5 h at room temperature, poured into saturated aqueous $NaHCO_3$, and extracted with $CHCl_3$. The combined organic layer was washed with brine, dried over $MgSO_4$, and concentrated in vacuo. The residue was purified by silica gel column chromatography (hexane−EtOAc (5:1)) to give (1S,4R)-N-[(9bS)-5-oxo-2,3,5,9b-tetrahydro-1H-pyrrolo[2,1-a]isoindol-9-yl]-4,7,7-trimethyl-3-oxo-2-oxabicyclo-[2,2,1]heptane-1-carboxamide (88 mg, 82%). mp 189 °C. ^{1}H NMR (300 MHz, $CDCl_3$): δ 1.01 (3H, s), 1.17 (3H, s), 1.19 (3H, s), 1.25−1.47 (1H, m), 1.73−1.82 (1H, m), 1.98−2.09 (2H, m), 2.22−2.33 (1H, m), 2.34−2.45 (2H, m), 2.58−2.69 (1H, m), 3.38−3.50 (1H, m), 3.66−3.78 (1H, m), 4.76 (1H, dd, J_1 = 10.2 Hz, J_1 = 5.9 Hz), 7.47 (1H, t, J = 8.0 Hz), 7.62 (1H, t, J = 8.0 Hz), 8.03 (1H, d, J = 8.0 Hz), 8.08 (1H, brs). HR-MS calcd for $C_{21}H_{25}N_2O_4$ (M+H)$^+$: 369.1814, found 369.1804. [α]$_D^{20}$ −92.4° (c 1.0, $CHCl_3$).

9-Amino-5H-pyrrolo[2,1-a]isoindol-5-one (23). To a stirred solution of **19** (100 mg, 0.47 mmol) in methyl alcohol (15 mL) were added Fe (powder, 200 mg) and then 6 N HCl (500 mL). The resultant mixture was stirred at room temperature for 30 min, poured into saturated aqueous $NaHCO_3$, and the aqueous layer was extracted with EtOAc. The combined organic layer was washed successively with water and brine, dried over $MgSO_4$, and concentrated in vacuo. The residue was purified by silica gel column chromatography (hexane−EtOAc (5:1)) to afford **23** (71 mg, 83%) as a red solid. mp 119−120 °C. ^{1}H NMR (300 MHz, $CDCl_3$): δ 3.85 (2H, brs), 6.02 (1H, d, J = 3.1 Hz), 6.17 (1H, t, J = 3.1 Hz), 6.78 (1H, d, J = 8.0 Hz), 6.99−7.04 (2H, m), 7.16 (1H, d, J = 8.0 Hz). MS (ESI+): m/z 185 (M+H)$^+$. HR-MS calcd for $C_{11}H_9N_2O$ (M+H)$^+$: 185.0715, found 185.0714.

9-Amino-3-(1-hydroxyvinyl)-5H-pyrrolo[2,1-a]isoindol-5-one (24). To a stirred solution of **20** (200 mg, 0.78 mmol) in MeOH−tetrahydrofuran (1:1, 20 mL) was added 10% Pd/C (25 mg), and the mixture was stirred at room temperature for 10 h under an atmospheric pressure of hydrogen. The catalyst was removed by filtration, and the filtrate was evaporated. The residue was purified by precipitation from EtOAc to yield **24** (208 mg, 100%) as a slightly green solid. mp 198−200 °C. ^{1}H NMR (300 MHz, DMSO-d_6): δ 5.92 (2H, brs), 6.29 (1H, d, J = 2.9 Hz), 6.62 (1H, s), 6.95 (1H, t, J = 5.2 Hz), 7.10 (2H, d, J = 5.2 Hz), 7.14 (1H, d, J = 2.9 Hz), 7.21 (1H, brs), 12.05 (1H, brs). MS (ESI+): m/z 227 (M+H)$^+$. HR-MS calcd for $C_{13}H_{11}N_2O_2$ (M+H)$^+$: 227.0821, found 227.0823.

Cyclin D−Cdk4 Assay. In vitro Cdk assays were performed as previously described[40] with some modifications. The recombinant human cyclin D_2−Cdk4 complex was expressed in Sf9 cells with a baculovirus expression system and then purified by HPLC. The purified cyclin D_2−Cdk4 was incubated with 50 μM ATP (0.5−1.5 μCi of [^{33}P]-ATP (3000 Ci/mmol)), 100 μM or 400 μM G1 peptide, R buffer (20 mM Tris-HCl pH 7.4, 10 mM $MgCl_2$, 4.5 mM 2-mercaptoethanol, 1 mM EGTA), and diluted compounds at 30 °C for 45 min. The reactions were terminated by addition of 350 mM H_3PO_4. Peptides were trapped and washed using P81 paper filter 96-well plates (Millipore) and 75 mM H_3PO_4. ^{33}P incorporation was measured with a Top Count (Packard).

References

(1) Pines, J. Cyclins and cyclin dependent kinases: take your partners. *Trends Biochem. Sci.* **1993**, *18*, 195−197.

(2) Sherr, C. J. D-type cyclins. *Trends Biochem. Sci.* **1995**, *20*, 187−190.

(3) (a) Taya, Y. Cell cycle-dependent phosphorylation of the tumor suppressor RB protein. *Mol. Cells* **1995**, *5*, 191−195. (b) Weinberg, R. A. The retinoblastoma protein and a cell cycle control. *Cell* **1995**, *81*, 323−330. (c) Kato, J.; Matsushime, H.; Hiebert, S. W.; Ewen, M. E.; Sherr, C. J. Direct binding of cyclin D to the retinoblastoma gene product (pRB) and pRB phosphorylation by the cyclin D-dependent kinase CDK4. *Genes Dev.* **1993**, *7*, 331−342. (d) Baldin, V.; Lukas, J.; Marcote, M. J.; Pagano, M.; Draetta, G. Cyclin D1 is nuclear protein required for cell cycle progression in G1. *Genes Dev.* **1993**, *7*, 812−821.

(4) Kamb, A. Cell-cycle regulators and cancer. *Trends Genet.* **1995**, *11*, 136−140.

(5) Akinaga, S.; Sugiyama, K.; Akiyama, T. UCN-01 (7-hydroxystaurosporine) and other indolocarbazole compounds: a new generation of anticancer agents for the new century? *Anti-Cancer Drug Des.* **2000**, *15*, 43−52.

(6) (a) Sedlacek, H. H.; Czech, J.; Naik, R.; Kaur, G.; Worland, P.; Losiewicz, M.; Parker, B.; Carlson, B.; Smith, A.; Senderowicz, A.; Sausville, E. Flavopiridol (L86-8275, NSC-649890), a new kinase inhibitor for tumor therapy. *Int. J. Oncol.* **1996**, *9*, 1143−1168. (b) Senderowicz, A. M.; Headlee, D.; Stinson, S. F.; Lush, R. M.; Kalil, N.; Villalba, L.; Hill, K.; Steinberg, S. M.; Figg, W. D.; Tompkins, A.; Arbuck, S. G.; Sausville, E. A. Phase I trial of continuous infusion flavopiridol, a novel cyclin-dependent kinase inhibitor, in patients with refractory neoplasms. *J. Clin. Oncol.* **1998**, *16*, 2986−2999.

(7) Glay, N. S.; Wodicka, L.; Thunnissen, A.-M.; Norman, T. C.; Kwon, S.; Espinoza, F. H.; Morgan, D. O.; Barnes, G.; Leclerc, S.; Meijer, L.; Kim, S.-H.; Lockhart, D. J.; Schultz, P. G. Exploiting chemical libraries, structure, and genomics in the search of kinase inhibitors. *Science* **1998**, *281*, 533−538.

(8) Barvian, M.; Boscheli, D.; Cossrow, J.; Dobrusin, E.; Fattaey, A.; Fritsch, A.; Fry, D.; Harvey, P.; Keller, P.; Garrett, M.; La, F.; Leopold, W.; McNamara, D.; Quin, M.; Trumpp-Kallmeyer, S.; Toogood, P.; Wu, Z.; Zhang, E. Prido[2,3-d]pyrimidin-7-one inhibitors of cyclin-dependent kinases. *J. Med. Chem.* **2000**, *43*, 4606−4616.

(9) Nugiel, D. A.; Etzkorn, A.-M.; Vidwans, A.; Benfield, P. A.; Boisclair, M.; Burton, C. R.; Cox, S.; Czerniak, P. M.; Doleniak, D.; Seitz, S. P. Indenopyrazoles as novel cyclin dependent kinase (CDK) inhibitors. *J. Med. Chem.* **2001**, *44*, 1334−1336.

(10) Fry, D. W.; Garret, M. D. Inhibitors of cyclin dependent kinases as therapeutic agents for the treatment of cancer. *Curr. Opin. Oncol. Endocr. Metab. Invest. Drugs* **2000**, *2*, 40−59.

(11) (a) Nicklaus, M. C.; Neamati, N.; Hong, H.; Mazumder, A.; Sunder, S.; Chen, J.; Milne, G. W. A.; Pommier, Y. HIV-1 integrase pharmacophore: discovery of inhibitors through three-dimensional database searching. *J. Med. Chem.* **1997**, *40*, 920−929. (b) Babine, R. E.; Bleckman, T. M.; Kissinger, C. R.; Showalter, R.; Pelletier, L. A.; Lewis, C.; Tucker, K.; Moomaw, E.; Parge, H. E.; Villafranca, J. E. Design, synthesis and X-ray crystallographic studies of novel FKBP-12 ligands. *Bioorg. Med. Chem. Lett.* **1995**, *5*, 1719−1724. (c) Shuker, S. B.; Hajduk, P. J.; Meadows, R. P.; Fesik, S. W. Discovering high-affinity ligands for proteins: SAR by NMR. *Science* **1996**, *274*, 1531−1534. (d) Manduskuie, T. P., Jr.; McNamara, K. J.; Ru, Y.; Knabb, R. M.; Stouten, F. W. Rational design and synthesis of novel, potent bis-phenylamidine carboxylate factor Xa inhibitors. *J. Med. Chem.* **1998**, *41*, 53−62. (e) Stewart, K. D.; Loren, S.; Frey, L.; Otis, E.; Klinghofer, V.; Hulkower, K. I. Discovery of a new cyclooxygenase-2 lead compound through 3-D database searching and combinatorial chemistry. *Bioorg. Med. Chem. Lett.* **1998**, *8*, 529−534. (f) Boehm, H.-J.; Boehringer, M.; Bur, D.; Gmuender, H.; Huber, W.; Klaus, W.; Kostrewa, D.; Kuehne, H.; Luebbers, T.; Meunier-Keller, N.; Mueller, F. Novel inhibitors of DNA gyrase: 3D structure based biased needle screening, hit validation by biophysical methods, and 3D guided optimization. A promising alternative to random screening. *J. Med. Chem.* **2000**, *43*, 2664−2674.

(12) Reviewed in (a) Desjarlais, R. L. Generation and use of three-dimensional databases for drug discovery. In *Practical Application of Computer-aided Drug Design*; Charifson, P. S., Ed.; Marcel Dekker: New York, 1997; pp 73−104. (b) Good, A. C.; Mason J. S. Three-dimensional structure database searches. In *Reviews in Computational Chemistry*; Lipkowitz, K. B., Boyd, D. B., Eds.; VCH Publishers: New York, 1996; pp 67−117.

(13) Reviewed in Murcko M. A. An introduction to *de novo* ligand design. In *Practical Application of Computer-aided Drug Design*; Charifson, P. S., Ed.; Marcel Dekker: New York, 1997; pp 304−354.

(14) Kuntz, I. D.; Blaney, J. M.; Oatley, S. J.; Langridge, R.; Ferrin, T. E. A geometric approach to macromolecule-ligand interactions. *J. Mol. Biol.* **1982**, *161*, 269.

(15) UNITY, developed and distributed by Tripos Associates, St. Louis, MO.

(16) Catalyst, developed by BioCAD and now distributed by Molecular Simulations Inc., Burlington, MA.

(17) (a) Nishibata, Y.; Itai, A. Automatic creation of drug candidate structures based on receptor structure. Starting point for artificial lead generation. *Tetrahedron* **1991**, *47*, 8985−90. (b) Nishibata, Y.; Itai, A. Confirmation of usefulness of a structure construction program based on three-dimensional receptor structure for rational lead generation. *J. Med. Chem.* **1993**, *36*, 2921−8.

(18) LeapFrog manual, SYBYL version 6.1, Tripos Associates, St. Louis, MO.

(19) Pearlman D. A.; Murcko M. A. CONCERTS-dynamic connection of fragments as an approach to *de novo* ligand design. *J. Med. Chem.* **1996**, *39*, 1651−1663.

(20) Clark, D. E.; Frenkel, D.; Levy, S. A.; Li, J.; Murray, C. W.; Robson, B.; Waszkowycz, B.; Westhead, D. R. PRO-LIGAND: an approach to *de novo* molecular design. 1. Application to the design of organic molecules. *J. Comput.-Aided Mol. Des.* **1995**, *9*, 13−32.

(21) (a) Boehm H. J. The computer program LUDI: a new method for the *de novo* design of enzyme inhibitors. *J. Comput.-Aided Mol. Des.* **1992**, *6*, 61−78. (b) Boehm H. J. LUDI: rule-based automatic design of new substituents for enzyme inhibitor leads. *J. Comput.-Aided Mol. Des.* **1992**, *6*, 593−606.

(22) Iwama, T.; Honma, T.; Ikeura, C. System for evaluation of availability of essential structures generated by *de novo* design programs (SEEDS). Unpublished results.

(23) De Bondt, H. L.; Rosenblatt, J.; Jancarik, J.; Jones, H.. D.; Morgan, D. O.; Kim, S.-H. Crystal structure of cyclin dependent kinase 2. *Nature* **1993**, *363*, 595−602.

(24) (a) Jeffrey, P. D.; Russo, A. A.; Polyak, K.; Gibbs, E.; Hurwitz, J.; Massague, J.; Pavletich, N. P. Mechanism of CDK activation revealed by the structure of a cyclin A-CDK2 complex. *Nature* **1995**, *376*, 313−20. (b) Russo, A. A.; Jeffrey, P. D.; Pavletich, N. P. Structural basis of cyclin dependent kinase activation by phosphorylation. *Nat. Struct. Biol.* **1996**, 3, 696−700. (c) Also see a review: Pavletich, N. P. Mechanism of cyclin dependent kinase regulation: structures of Cdks, their cyclin activators, and cip and ink4 inhibitors. *J. Mol. Biol.* **1999**, *287*, 821−828.

(25) (a) Russo, A. A.; Tong, L.; Lee, J.-O.; Jeffrey, P. D.; Pavletich, N. P. Structural basis for inhibition of the cyclin dependent kinase Cdk6 by the tumor suppressor p16INK4a. *Nature* **1998**, *395*, 237−243. (b) Jeffrey, P. D.; Tong, L.; Pavletich, N. P. Structural basis of inhibition of CDK-cyclin complexes by INK4 inhibitors. *Genes Dev.* **2000**, *14*, 3115−3125. (c) Brotherton, D. H.; Dhanaraj, V.; Wick, S.; Leonardo, B.; Domaille, P. J.; Volyanik, E.; Xu, X.; Parisini, E.; Smith, B. O.; Archher, S. J.; Serrano, M.; Brenner, S. L.; Blundell, T. L.; Laue, E. D. Crystal structure of the complex of the cyclin D-dependent kinase Cdk6 bound to the cell-cycle inhibitor p19INK4d. *Nature* **1998**, *395*, 244−250.

(26) (a) http://www.nih.go.jp/mirror/Kinases/pkr/pk_catalytic/pk_hanks_seq_align_long.html. (b) Hanks, S. K.; Quinn, A. M.; Hunter, T. The protein kinase family: conserved features and deduced phylogeny of the catalytic domains. *Science* **1988**, *241*, 42−52. (c) Hanks, S. K.; Quinn, A. M. Protein kinase catalytic domain sequence database: identification of conserved features of primary structure and classification of family members. *Methods Enzymol.* **1991**, *200*, 38−62. (d) Hanks, S. K.; Hunter, T. Protein kinases. 6. the eukaryotic protein kinase superfamily: kinase (catalytic) domain structure and classification. *FASEB J.* **1995**, *9*, 576−96.

(27) BIOCES[E], developed by NEC Co., Tokyo, Japan.

(28) Brooks, B. R.; Bruccoleri, R. E.; Olafson, B. D.; States, D. J.; Swaminathan, S.; Karplus, M. CHARMM: a program for macromolecular energy, minimization, and dynamic calculation. *J. Comput. Chem.* **1983**, *4*, 187−217.

(29) de Azevedo, W. F., Jr.; Mueller-Dieckmann, H.-J.; Schulze-Gahmen, U.; Worland, P. J.; Sausville, E.; Kim, S.-H. Structural basis for specificity and potency of a flavonoid inhibitor of human CDK2, a cell cycle kinase. *Proc. Natl. Acad. Sci. U.S.A.* **1996**, *93*, 2735−40.

(30) Lawrie, A. M.; Noble, M. E. M.; Tunnah, P.; Brown, N. R.; Johnson, L. N.; Endicott, J. A. Protein kinase inhibition by staurosporine revealed in details of the molecular interaction with CDK2. *Nat. Struct. Biol.* **1997**, *4*, 796−801.

(31) De Azevedo, W. F., Jr.; Leclerc, S.; Meijer, L.; Havlicek, L.; Strnad, M.; Kim, S.-H. Inhibition of cyclin Dependent kinases by purine analogs. Crystal structure of human cdk2 complexed with roscovitine. *Eur. J. Biochem.* **1997**, *243*, 518−526.

(32) Russo, A. A.; Jeffrey, P. D.; Patten, A. K.; Massague, J.; Pavletich, N. P. Crystal structure of the p27Kip1 cyclin dependent-kinase inhibitor bound to the cyclin A-Cdk2 complex. *Nature* **1996**, *382*, 325−331.

(33) Meijer, L.; Thunnissen, A. M. W. H.; White, A. W.; Garnier, M.; Nikolic, M.; Tsai, L. H.; Walter, J.; Cleverley, K. E.; Salinas, P. C.; Wu, Y. Z.; Biernat, J.; Mandelkow, E. M.; Kim, S. H.; Pettit, G. R. Inhibition of cyclin dependent kinases, GSK-3b and CK1 by hymenialdisine, a marine sponge constituent. *Chem. Biol.* **2000**, *7*, 51−63.

(34) Sequential buildup methods fall into the following two categories: atom-by-atom approaches and fragment-by-fragment approaches. In atom-by-atom approaches, ligands are constructed atom by atom. Murcko M. A. An introduction to *de novo* ligand design. In *Practical Application of Computer-aided Drug Design*; Charifson, P. S., Ed.; Marcel Dekker: New York, 1997; pp 322−325.

(35) The available chemicals directory distributed by MDL Information Systems, San Leandro, CA.

(36) QUANTA modeling environment, December 1998; Molecular Simulations Inc.: San Diego, CA, 1998.

(37) Grigg, R.; Sridharan, V.; Stevenson, P.; Sukirthanlingam, S.; Worakun, T. The synthesis of fused ring nitrogen heterocycles via regiospecific intramolecular Heck reactions. *Tetrahedron* **1990**, *46*, 4003−4018.

(38) Ikuta, M.; Kamata, K.; Fukasawa, K.; Honma, T.; Machida, T.; Hirai, H.; Suzuki-Takahashi, I.; Hayama, T.; Nishimura, S. Crystallographic approach to identification of cyclin dependent kinase 4 (CDK4) specific inhibitors by using CDK4 mimic CDK2 protein. *J. Biol. Chem.* **2001**, *276*, 27548−27554.

(39) We investigated the following kinases: PKA, PKC, PKBα (Akt-1), CaMK II, p38α, ERK1, MEK1, Src, Lck, Flt-1, ZAP, EGFR, FGFR1, and PDGFRβ. Honma, T.; Yoshizumi, T.; Hashimoto, K.; Hayashi, N.; Kawanishi, N.; Fukasawa, K.; Takaki, T.; Ikeura, C.; Ikuta, M.; Suzuki-Takahashi, I.; Hayama, T.; Nishimura, S.; Morishima, H. A novel approach for the development of selective Cdk4 inhibitors: library design based on locations of Cdk4 specific amino acid residues. *J. Med. Chem.* 2001, 44, 4628−4640.

(40) (a) Kitagawa, M.; Okabe, T.; Ogino, H.; Matsumoto, H.; Suzuki-Takahashi, I.; Kokubo, T.; Higashi, H.; Saitoh, S.; Taya, Y.; Yasuda, H.; Ohba, Y.; Nishimura, S.; Tanaka, N.; Okuyama, A. Butyrolactone I, a selective inhibitor of cdk2 and cdc2 kinase. *Oncogene* **1993**, *8*, 2425−2432. (b) Kitagawa, M.; Higashi, H.; Jung, H.-K.; Suzuki-Takahashi, I.; Ikeda, M.; Tamai, K.; Kato, J.; Segawa, K.; Yoshida, E.; Nishimura, S.; Taya, Y. The consensus motif for phosphorylation by cyclin D1-Cdk4 is different from that for phosphorylation by cyclin A/E-Cdk2. *EMBO J.* **1996**, *15*, 7060−7069.